Superconductor-insulator transition in two-dimensional dirty boson systems

Mats Wallin
Department of Theoretical Physics, Royal Institute of Technology, S-100 44 Stockholm, Sweden

Erik S. Sørensen
Department of Physics, University of British Columbia, Vancouver, British Columbia, Canada V6T 1Z1

S. M. Girvin
Department of Physics, Indiana University, Bloomington, Indiana 47405

A. P. Young
Department of Physics, University of California, Santa Cruz, California 95064
(Received 22 September 1993; revised manuscript received 18 January 1994)

Universal properties of the zero-temperature superconductor-insulator transition in two-dimensional amorphous films are studied by extensive Monte Carlo simulations of bosons in a disordered medium. We report results for both short-range and long-range Coulomb interactions for several different points in parameter space. In all cases we observe a transition from a superconducting phase to an insulating Bose glass phase. From finite-size scaling of our Monte Carlo data we determine the universal conductivity σ^* and the critical exponents at the transition. The result $\sigma^* = (0.55 \pm 0.06)(2e)^2/h$ for bosons with long-range Coulomb interaction is roughly consistent with experiments reported so far. We also find $\sigma^* = (0.14 \pm 0.03)(2e)^2/h$ for bosons with short-range interactions.

I. INTRODUCTION

From the work of Abrahams, Anderson, Licciardello, and Ramakrishnan[1] it is known that no true metallic behavior can be observed for noninteracting electrons at $T = 0$ in two dimensions, since all states will be localized by arbitrarily weak disorder. When repulsive interactions are turned on the situation is less clear but the general belief[2] is that a metallic phase still should be absent at $T = 0$ in the presence of disorder, although we know of no rigorous proof of this. However, in the presence of attractive interactions, a superconducting phase is expected,[3] both at $T = 0$ and finite T, even for a finite amount of disorder, because disorder is irrelevant[4] at the finite-temperature transition, which is of the Kosterlitz-Thouless[5] type discussed below. The onset of superconductivity at $T = 0$ is presumed then, in $d = 2$, to be directly from the insulating phase with no intervening metallic phase. One should therefore in principle be able to observe a direct insulator-superconductor transition at zero temperature in two dimensions as a function of disorder and/or interaction strength. The main topic of this paper is to analyze such a transition and extract its universal features.

Dimensionality and divergent length scales play an important role in continuous phase transitions. The diverging correlation length scale implies that many microscopic details are irrelevant. Furthermore physical quantities containing dimensions of length to some nonzero power typically diverge or vanish at the critical point. Two dimensions (2D) is a special case in that the conductivity contains no length scale units; i.e., the conductance per square is the same as the conductivity. Hence, right at the $T = 0$ quantum critical point, the conductivity is not only finite and nonzero but also *universal*,[6,7] even though it is zero in the insulating phase and infinite in the superconducting phase. This view differs from that of previous work[8] which parametrized the transition in terms of the *normal* state resistivity. The calculation of this universal conductivity is one of the main goals of the present paper. A short account on some of our results has already been published.[9]

A schematic phase diagram is shown in Fig. 1 as a function of temperature, T, and disorder, Δ. At zero temperature, a critical amount of disorder, Δ_c, separates the superconducting from the insulating phase. Even at finite temperatures the superconducting phase persists whereas a truly insulating phase only exists at $T = 0$, because, at finite T, electrons can be *inelastically* scattered from one localized state to another, and hence conduct. This insulating phase, consisting of localized electron pairs, can then be described, close to the critical point, as a Bose-condensed fluid of vortices. The universality class of the transition should therefore be that of the superconductor to Bose glass.[10]

Let us first discuss the nature of the transition at finite temperatures indicated by the solid line in Fig. 1. The finite-temperature transition should have many similarities with the 2D XY transition at which logarithmically interacting vortices unbind.[5] However, Pearl[11] showed that in a superconducting film vortex pairs only have logarithmic interactions out to a distance $\Lambda_\perp = 2\lambda^2/d$ beyond which the interaction energy falls off as $1/r$. Here λ is the bulk penetration depth, d the film thick-

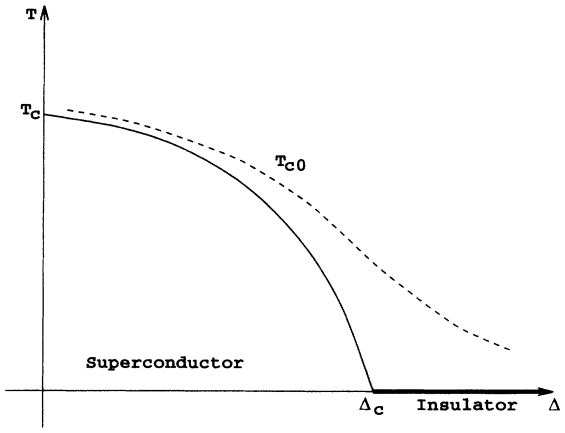

FIG. 1. Sketch of the general phase diagram for thin-film superconductors as a function of disorder, Δ, and temperature, T. The dashed line, T_{c0}, indicates the mean-field onset temperature where Cooper pairs start to form. At $T = 0$ an insulating phase appears (solid line) and a transition from a superconductor to an insulator takes place at a critical value of the disorder Δ_c.

ness, and $\Lambda_\perp$ the screening length for magnetic fields. Due to this cutoff, the energy required to create a vortex is always *finite* and no sharp transition should exist. However, according to the Kosterlitz-Thouless theory,[5] the value of $\Lambda_\perp(T_c)$ is given *exactly* by[12–14] $\Lambda_\perp(T_c) = \phi_0^2/(16\pi^2 k_B T_c)$, where $\phi_0 = hc/2e$ is the flux quantum. Numerically $\Lambda_\perp(T_c) = 2/T_c$ where T_c is in kelvin and $\Lambda_\perp(T_c)$ is in *centimeters*. Thus, $\Lambda_\perp$ is so large at T_c that rounding of the transition due to the presence of free vortices below T_c is almost certainly unobservable. In fact, rounding due to finite-size effects is probably more important.

The vortex unbinding transition at T_c is driven by fluctuations in the phase of the superconducting order parameter. At a higher temperature, T_{c0}, fluctuations in the amplitude of the order parameter will become important and a crossover to a regime dominated by paraconductivity[15] will occur. T_{c0} is indicated by the dashed line in Fig. 1. For $T_c \leq T \ll T_{c0}$ the presence of free vortices destroys the characteristic global properties of the superconducting phase. Nevertheless, a *local* order parameter still exists between T_c and T_{c0}. The presence of free vortices leads to a finite conductivity of the form[12] $\sigma_v \sim 0.37\sigma_n(\xi/\xi_c)^2$, where σ_n is the conductivity of the normal state electrons, ξ_c the core size of a vortex, and ξ, a typical distance between free vortices, is the Kosterlitz-Thouless[5] correlation length which diverges exponentially at T_c. The exponential tail in the resistivity caused by the presence of free vortices between T_c and T_{c0} has been observed experimentally[16,17] in superconducting films with high normal state resistivity. In these experiments the "mean field onset temperature" T_{c0} is determined by fitting the resistance to an Aslamazov-Larkin[18] form, and $T_{c0} - T_c$ is found to be of the order of half a kelvin. In the dirty limit, Beasley *et al.*[14] derive the relationship $\tau_c \equiv (T_{c0} - T_c)/T_c \sim 0.17e^2/\sigma_n\hbar$, and so, for films with a relatively high sheet resistance, τ_c can be appreciable. For a review of the finite-temperature transition we refer the reader to Ref. 19. More recently some evidence for a vortex-antivortex unbinding transition in superconducting niobium films[20] with $R_\square = 122\ \Omega$ has been found. However, the difference between T_c and T_{c0} is very small in the clean limit which makes the Kosterlitz-Thouless behavior difficult to observe.

The superconducting order parameter is a complex scalar, described by both a magnitude and a phase. Our key basic assumption is that universal properties at superconductor-insulator transition are determined only by phase fluctuations, as outlined above, and that the magnitude of the order parameter, and therefore of the gap in the fermionic energy spectrum, remains finite at the critical point. We thus assume that when disorder drives T_c to zero, T_{c0} remains nonzero. If the transition is approached from the insulating side, a local order parameter appears before the onset of global phase coherence at Δ_c. Implicit in our assumption is that Cooper pairs, and thus a gap to fermionic excitations, persists into the insulating phase, even though superconductivity is destroyed by phase fluctuations. On the scale of a diverging *phase*-correlation length, ξ, the individual Cooper pairs will look like point particles. The fermionic degrees of freedom should therefore be highly suppressed at the critical point and an approximate description in terms of point-like bosons should be valid. It is possible that strong disorder destroys the local fermionic gap at a finite density of points, but, provided that the Fermi degrees of freedom are localized, they may still be dynamically irrelevant and our model applicable.

Since we shall be concerned with the transition at $\Delta = \Delta_c$, $T = 0$, vortices in the system will not be excited thermally, but there will be vortices present created by quantum fluctuations.[21] We therefore need to treat the vortices as quantum mechanical objects and one might expect the transition at Δ_c to be described by a (2+1)D XY model,[22] where the extra dimension arises because we are considering a T=0 quantum phase transition; see, e.g., Ref. 10. However, as we shall see in Sec. II, although the physics is indeed described by a (2+1)D system, its symmetry is, in general, *not* that of the XY model. It is also worth noting that the vortex mobility, $(2e^2/\pi\hbar^2)\xi^2 R_\square$,[19] is significantly augmented in dirty superconducting films. Hence, at Δ_c the vortices should be seen as fairly light objects that move rather freely. At still higher disorder the Bose glass phase should cross over into a Fermi glass when the individual electrons constituting the bosons become localized. This behavior may have already been observed in a magnetic field.[23]

Recent experiments[24] seem to confirm that a direct insulator-superconductor transition indeed does take place at zero temperature in many materials. Haviland *et al.*[25] and Liu *et al.*[26] have performed experiments on Bi films grown *in situ*. The experimental technique is described in Ref. 27. These films are believed to be truly amorphous on an atomic scale. The authors report a critical dc resistivity, $R_\square^*$, very close to R_Q, where

$$R_Q = h/4e^2 \approx 6453\ \Omega\ . \tag{1.1}$$

Furthermore, experiments performed on DyBaCuO

films[28,29] and NdCeCuO (Ref. 30) show clear evidence for a direct superconductor-insulator transition. The reported critical resistivity seems in this case to be somewhat higher, around 10 kΩ or $1.5R_Q$.[28,29] Lee and Ketterson[31] have presented results from experiments on MoC films again showing very clear evidence for a superconductor-insulator transition occurring at zero temperature, but with $R^*_\square$ slightly lower, in the range 2.8–3.5 kΩ $\sim 0.5R_Q$. Furthermore, experiments performed on Josephson junction arrays,[32,33] which are believed to be in the same universality class, also seem to support the picture of a superconductor-insulator transition in agreement with theory.[34–36] The existence of a superconductor-insulator transition in two-dimensional films at zero temperature thus seems well established but evidence for the universality of the critical resistivity remains weak. It is not clear, however, whether all the experiments are in the critical region. In order to establish that a given experiment is actually probing the critical regime, one must show scaling of the resistivity data. This has been done successfully by Hebard and Paalanen[37,38] for the field-tuned transition and partially successfully by the Minnesota group.[39] However, it is likely that most measurements to date have failed to probe the critical regime, and further experiments at even lower temperatures are expected to give better agreement among the different estimates of $R^*_\square$.

The situation concerning the relevance of a bosonic picture seems less clear. Hebard and Paalanen[37,38] have reported results on amorphous InO films in a magnetic field, supporting the existence of Cooper pairs in the insulating phase. For the $B = 0$ transition, Hebard and Paalanen[40] have presented clear transport evidence that T_{c0} remains finite as T_c is driven to zero. On the other hand, direct tunneling measurements by Dynes *et al.*[41] and Valles *et al.*[42] on homogeneously disordered Pb films shows that the gap goes to zero at the critical point. There seems, however, to be a general agreement that a local superconducting order parameter exists prior to the transition in granular films and in Josephson junction arrays where the individual grains become superconducting above T_c. It is possible that tunneling experiments tend to emphasize regions of the samples containing quasilocalized fermion states below the gap which are necessary to achieve tunneling.

A number of theoretical and numerical studies of the superconductor-insulator transition have been performed. Gold[43] studied the impurity-induced insulating transition in the interacting Bose gas. Giamarchi and Schulz[44] considered the one-dimensional electron gas with attractive interactions in the presence of disorder. They found a transition to a localized phase in the same universality class as that of repulsively interacting bosons in a random potential. This lends strong support to our assumption of the dirty boson universality class in the 2D case. Fisher *et al.*[45–47,10] considered the boson Hubbard model and, through a scaling analysis, derived equations for the exponents governing the superconductor-insulator transition as well as the phase diagram for dirty bosons. A renormalization group approach was taken by Weichman *et al.*[48] who performed a double-ε expansion for the dirty boson problem. Following the initial suggestion of a Bose glass phase in the disordered system and a Mott insulator in the clean system, Batrouni *et al.*[49] and Krauth and Trivedi[50] showed, by quantum Monte Carlo simulations, the existence of Mott insulating phases in an interacting boson system without disorder, characterized by the exponents predicted by Fisher *et al.*[10] Subsequently, these authors considered the disordered case and evidence for a Bose glass was found.[51,52] A Bose glass phase was also observed in a real space renormalization group study by Singh and Rokhsar.[53] The universal conductivity was first calculated by a $1/N$ expansion and Monte Carlo methods for the (2+1)D XY model by Cha *et al.*[54] and Girvin *et al.*[55,56] The universal conductivity for disordered bosons was then calculated by Runge[57] by exact diagonalization techniques on small lattices. Universal properties for a boson system in the presence of disorder both with and without long-range interactions were calculated by Sørensen *et al.*[9,58] by Monte Carlo simulations, using a path integral representation which, effectively, only includes phase fluctuations in the Bose field. A universal conductivity was also recently found by Kampf and Zimanyi[59] in the boson Hubbard model including both phase and amplitude fluctuations. Two recent works have recently been published after the present work was finished. Batrouni *et al.*[60] have calculated the universal conductivity by quantum Monte Carlo simulations directly on the boson Hubbard model, and Makivić *et al.*[61] have calculated the exponents and the universal conductivity using a hard-core boson model. The results of these last two papers differ from ours, and we shall comment on this in Sec. VIII.

Here we shall consider two forms of interaction between the bosons: short-range repulsive interaction and long-range Coulomb interaction. The model with short-range interactions is relevant to experiments on the onset of superfluidity in ^{4}He films.[54] However, our present results for the zero-temperature transition in 2D are not directly applicable to He experiments in porous media such as Vycor or xerogel,[62,63] since these experiments are mainly concerned with the 3D transition at finite temperatures. As stated above, the model with Coulomb interactions is expected to be in the correct universality class to describe the superconductor-insulator transition. However, the model and many of the results presented in this paper are applicable to other systems too. The world lines of the dirty boson model describe a gas of stringlike objects in a random medium. In addition to the superconductor-insulator transition this model may also apply to other problems such as vortex lines in high-temperature superconductors with correlated pinning centers[64,65] and polymer solutions. Our results for *universal* quantities might also be relevant for these problems.

The organization of the paper is as follows. In Sec. II we shall construct a form of the boson Hubbard model, including disorder and interactions, which is suitable for Monte Carlo simulations. Here we shall assume, as discussed above, that only bosonic degrees of freedom, i.e., complex order parameter fluctuations, are relevant at the superconductor-insulator transition. In addition, to further simplify the numerical work, we effectively include

only phase fluctuations of the bosons, amplitude fluctuations being neglected. Section III describes the scaling theory of the quantities that we are interested in. We discuss, in Sec. IV, how we determine these quantities in the simulation, and we also treat the finite-size scaling techniques needed to extrapolate our results to infinite size. Section V describes our Monte Carlo methods, while Sec. VI presents our results for short-range interactions and disorder, relevant to experiments on helium films. In Sec. VII long-range Coulomb interactions are included along with disorder. We believe that this model contains all ingredients necessary to make it relevant to experiments on the superconductor-insulator transition, i.e., that it is in the correct universality class. Our results are discussed in Sec. VIII.

II. THE MODEL

In this section we introduce our basic model and via a sequence of transformations arrive at a form suitable for Monte Carlo simulation. As argued above it should be possible to describe the universal features of the superconductor-insulator transition in terms of boson physics. In this section we shall argue that the relevant starting point is the boson Hubbard model with a random local chemical potential (site energy). If only phase fluctuations are relevant we can map this model onto a dual Villain type model. We shall see that only in the absence of disorder and when there is an integer number of bosons per site does this model belong to the same universality class as the (2+1)D XY model.

In order to model the superconductor-insulator transition in terms of bosons, we must include an on-site repulsive interaction; otherwise all bosons would collapse into the lowest lying, highly localized state. The on-site repulsion term is the simplest possible way to model Coulomb repulsion. The correct treatment of the long-range part of the interaction will be discussed below. For simplicity we shall take an underlying square lattice of spatial size $N = L \times L$. Changes in the symmetry of the lattice are not expected to modify the critical behavior of the model. We can then write down the boson Hubbard model the in the presence of disorder:[10,47,66]

$$H_{\rm bH} = H_0 + H_1, \tag{2.1}$$

where

$$H_0 = \frac{U}{2}\sum_{\mathbf{r}} \hat{n}_{\mathbf{r}}^2 - \sum_{\mathbf{r}} (\mu + v_{\mathbf{r}} - zt)\hat{n}_{\mathbf{r}},$$
$$H_1 = -t \sum_{\langle \mathbf{r},\mathbf{r}'\rangle} (\hat{\Phi}_{\mathbf{r}}^\dagger \hat{\Phi}_{\mathbf{r}'} + \hat{\Phi}_{\mathbf{r}} \hat{\Phi}_{\mathbf{r}'}^\dagger) \ . \tag{2.2}$$

Here U is the on-site repulsion, μ is the chemical potential, z the number of nearest neighbors, and $v_{\mathbf{r}}$ represents the random on-site potential varying uniformly in space between $-\Delta$ and Δ. As usual, $\hat{n}_{\mathbf{r}} = \hat{\Phi}_{\mathbf{r}}^\dagger \hat{\Phi}_{\mathbf{r}}$ is the number operator on site $\mathbf{r}$. The hopping strength is given by t, and $\langle \mathbf{r}, \mathbf{r}' \rangle$ denotes summation over pairs of nearest neighbors, each pair counted once.

In the absence of disorder there is no insulating phase unless we fix the boson density at an integer value, n_0. Let us consider this case first. If we set $\hat{\Phi}_{\mathbf{r}} \equiv |\hat{\Phi}_{\mathbf{r}}| e^{i\hat{\theta}_{\mathbf{r}}}$ and integrate out amplitude fluctuations, the boson Hubbard model, Eq. (2.2), becomes a model of coupled Josephson junctions,[10,45] (see also the Appendix),

$$H_{\rm JJ} = \frac{U}{2}\sum_i \hat{n}_{\mathbf{r}}^2 - \sum_{\langle \mathbf{r},\mathbf{r}'\rangle} t\cos(\hat{\theta}_{\mathbf{r}} - \hat{\theta}_{\mathbf{r}'}) \ , \tag{2.3}$$

where, in this representation, $\hat{n}_{\mathbf{r}}$, which denotes the deviation of the boson number from n_0, runs from $-\infty$ to ∞ and so Eq. (2.3) can only be quantitatively compared with the Hubbard model, Eq. (2.2), when n_0 is very large, but is expected to be in the same universality class for arbitrary integer n_0. Note that t in Eq. (2.3) is $2n_0$ times the parameter t in Eq. (2.2). The phase operator, $\hat{\theta}_{\mathbf{r}}$ is canonically conjugate to $\hat{n}_{\mathbf{r}}$, and so this version of the boson Hubbard model can be written in the angle representation as the quantum rotor model[54,45,10,67]

$$H_{\rm qr} = \frac{U}{2}\sum_{\mathbf{r}} \left(\frac{1}{i}\frac{\partial}{\partial\theta_{\mathbf{r}}}\right)^2 - \sum_{\langle \mathbf{r},\mathbf{r}'\rangle} t\cos(\theta_{\mathbf{r}} - \theta_{\mathbf{r}'}) \ . \tag{2.4}$$

Let us write the partition function corresponding to $H_{\rm qr}$ as

$$Z = {\rm Tr}\, \exp[-\beta(T+V)] \ , \tag{2.5}$$

where the kinetic energy of the rotors is

$$T = -\frac{U}{2}\sum_{\mathbf{r}} \frac{\partial^2}{\partial\theta_{\mathbf{r}}^2} \tag{2.6}$$

(which corresponds to the potential energy of the bosons) and the potential energy of the rotors is

$$V = -\sum_{\langle \mathbf{r},\mathbf{r}'\rangle} t\cos(\theta_{\mathbf{r}} - \theta_{\mathbf{r}'}) \ . \tag{2.7}$$

We evaluate the trace in the partition function by writing a path integral over M time slices τ_j between $\tau = 0$ and $\tau = \beta$:

$$Z = {\rm Tr}\,\{\exp[-\beta(T+V)]/M\}^M$$
$$= \lim_{M\to\infty} {\rm Tr}\,\{\exp[-\Delta\tau\ T]\exp[-\Delta\tau V]\}^M \ , \tag{2.8}$$

where $\hbar\tau$ is imaginary time and

$$\Delta\tau = \beta/M \tag{2.9}$$

is the width of one time slice. Note that the limit $\Delta\tau \to 0$ must be taken to correctly represent the underlying quantum mechanics problem. Equation (2.8) can be rewritten by inserting complete sets of states

$$Z \approx \int \mathcal{D}\theta \prod_{j=0}^{M-1} \langle\{\theta(\tau_{j+1})\}|\exp[-\Delta\tau T] \times \exp[-\Delta\tau V]|\{\theta(\tau_j)\}\rangle \ , \tag{2.10}$$

where $|\{\theta(\tau_j)\}\rangle$ is a coherent state in which site $\mathbf{r}$ has phase $\theta_{\mathbf{r}}(\tau_j)$ at time τ_j and the trace is enforced by pe-

riodic boundary conditions

$$\{\theta(\tau_M)\} = \{\theta(\tau_0)\} \ . \tag{2.11}$$

The coherent states are eigenstates of the potential, and so

$$\exp[-\Delta\tau V]\left|\{\theta(\tau_j)\}\right\rangle = \exp\left\{\Delta\tau t \sum_{\langle \mathbf{r},\mathbf{r}'\rangle} \cos\left[\theta_{\mathbf{r}'}(\tau_j) - \theta_{\mathbf{r}}(\tau_j)\right]\right\}\left|\{\theta(\tau_j)\}\right\rangle \ , \tag{2.12}$$

where the sum is over all nearest neighbor spatial pairs, and hence Eq. (2.10) becomes

$$Z \approx \int \mathcal{D}\theta \prod_{j=0}^{M-1} \exp\left\{K_x \sum_{\langle \mathbf{r},\mathbf{r}'\rangle} \cos[\theta_{\mathbf{r}'}(\tau_j) - \theta_{\mathbf{r}}(\tau_j)]\right\} T_j \ , \tag{2.13}$$

where

$$T_j \equiv \langle\{\theta(\tau_{j+1})\}|e^{-\Delta\tau T}|\{\theta(\tau_j)\}\rangle \tag{2.14}$$

and

$$K_x = t\Delta\tau \ . \tag{2.15}$$

Since the kinetic energies on different sites commute, we can consider each site separately:

$$T_j = \prod_{\mathbf{r}} \left\langle \theta_{\mathbf{r}}(\tau_{j+1}) \left| \exp\left[\frac{\Delta\tau U}{2}\frac{\partial^2}{\partial\theta_{\mathbf{r}}^2}\right] \right| \theta_{\mathbf{r}}(\tau_j)\right\rangle \ . \tag{2.16}$$

Let $J_{\mathbf{r}}^{\tau}(\tau_j)$ be the integer-valued angular momentum at $\mathbf{r}$ at time τ_j. The corresponding state has the wave function

$$\langle\theta_{\mathbf{r}}(\tau_j)|J_{\mathbf{r}}^{\tau}(\tau_j)\rangle = e^{iJ_{\mathbf{r}}^{\tau}(\tau_j)\theta_{\mathbf{r}}(\tau_j)} \ , \tag{2.17}$$

which is an eigenfunction of the kinetic energy. Inserting this complete set of states, we have

$$T_j = \sum_{\{J\}} \prod_{\mathbf{r}} \left\langle \theta_{\mathbf{r}}(\tau_{j+1})|J_{\mathbf{r}}^{\tau}(\tau_j)\right\rangle \exp\left\{-\frac{\Delta\tau U}{2}[J_{\mathbf{r}}^{\tau}(\tau_j)]^2\right\} \times \left\langle J_{\mathbf{r}}^{\tau}(\tau_j)|\theta_{\mathbf{r}}(\tau_j)\right\rangle \tag{2.18}$$

and thus

$$Z \approx \int \mathcal{D}\theta \sum_{\{J\}} \exp\left\{K_x \sum_{\langle \mathbf{r},\mathbf{r}'\rangle} \sum_{j=0}^{M-1} \cos\left[\theta_{\mathbf{r}'}(\tau_j) - \theta_{\mathbf{r}}(\tau_j)\right]\right\} \times \exp\left\{-\frac{\Delta\tau U}{2}\sum_{\mathbf{r}}\sum_{j=0}^{M-1}[J_{\mathbf{r}}^{\tau}(\tau_j)]^2\right\} \times \exp\left\{i\sum_{\mathbf{r}}\sum_{j=0}^{M-1} J_{\mathbf{r}}^{\tau}(\tau_j)\left[\theta_{\mathbf{r}}(\tau_j) - \theta_{\mathbf{r}}(\tau_{j+1})\right]\right\} . \tag{2.19}$$

We can now proceed in two possible ways. We can either integrate out the angular variables $\{\theta\}$ to obtain a statistical mechanics problem in the integer variables $\{J\}$, or we can sum over the $\{J\}$ to obtain a classical (2+1)-dimensional XY model. Let us start with the latter.

Because $\Delta\tau$ is small, the sum over the $\{J\}$ is slowly convergent. We may remedy this by using the Poisson summation formula

$$F(\theta) \equiv \sum_J e^{-\Delta\tau U J^2/2} e^{iJ\theta} = \sum_{m=-\infty}^{\infty} \int_{-\infty}^{+\infty} dJ\, e^{2\pi i J m} e^{-\Delta\tau U J^2/2} e^{iJ\theta} = \sum_{m=-\infty}^{\infty} \sqrt{\frac{2\pi}{\Delta\tau U}} e^{-\frac{1}{2\Delta\tau U}(\theta - 2\pi m)^2} \ . \tag{2.20}$$

This periodic sequence of narrow Gaussians is the Villain approximation[68] to the periodic function

$$F(\theta) \approx e^{K_\tau \cos(\theta)} \ , \tag{2.21}$$

where we have dropped an irrelevant constant prefactor, and

$$K_\tau \equiv \frac{1}{U\Delta\tau} \ . \tag{2.22}$$

Using this result in Eq. (2.19) we finally arrive at the partition function of the anisotropic (2+1)D classical XY model,

$$Z = \int \mathcal{D}\theta \exp\left\{\sum_{\langle \mathbf{l},\mathbf{l}'\rangle} K_{\langle \mathbf{l},\mathbf{l}'\rangle} \cos(\theta_{\mathbf{l}'} - \theta_{\mathbf{l}})\right\} \ , \tag{2.23}$$

where the sum is now over all near-neighbor bonds in both the space and time directions, i.e. $\mathbf{l} = (x, y, \tau)$. For spatial bonds,

$$K_{\mathbf{l},\mathbf{l}'} = K_x \ , \tag{2.24}$$

given by Eq. (2.15), while for temporal bonds

$$K_{\mathbf{l},\mathbf{l}'} = K_\tau \ , \tag{2.25}$$

given by Eq. (2.22). It is implicitly assumed here that the difference between the Villain action and the cosine term (which is small for small $\Delta\tau$) is in fact irrelevant in the renormalization group sense.

Note that we need to take the limit $\Delta\tau \to 0$ which implies $K_x \to 0$ and $K_\tau \to \infty$ such that the geometric mean

$$K = (K_x K_\tau)^{1/2} = \frac{t}{U} \tag{2.26}$$

is finite. Universality properties are unaffected[69] if we rescale space and time so that we obtain finally an *isotropic* (2+1)D XY model

$$Z = \int \mathcal{D}\theta \exp\left\{ K \sum_{\langle \mathbf{l},\mathbf{l}' \rangle} \cos(\theta_{\mathbf{l}'} - \theta_{\mathbf{l}}) \right\} . \tag{2.27}$$

We are interested in the behavior of the boson Hubbard model at $T = 0$, which means taking the number of time slices, M, to infinity. The coupling constant, K, then controls the quantum rather than thermal fluctuations.[67,21]

Allowing for a noninteger boson density and/or including the random potential in the boson Hubbard model, Eq. (2.2), makes the model more realistic but complicates the situation by breaking the particle-hole symmetry of the bosons. This corresponds to broken time-reversal symmetry for the quantum rotors (since particle number is represented by angular momentum) and hence leads to *complex* weights in the corresponding classical statistical mechanical problem[46] which is no longer in the universality class of the (2+1)D XY model. The difficulty of complex weights can be avoided by considering the alternative approach to Eq. (2.19) in which we integrate out the $\{\theta\}$ variables. Let us do this first for the case of integer boson density and no disorder. Adding the effects of disorder and noninteger density will then be easy and will lead to a *real* action.

We first reexpress the cosine in Eq. (2.19) as the best Villain approximation to it, i.e.,

$$\exp(K_x \cos\theta) \longrightarrow \sum_{m=-\infty}^{\infty} \exp\left\{ -\frac{1}{2\tilde{K}_x}(\theta - 2\pi m)^2 \right\} . \tag{2.28}$$

To determine $\tilde{K}_x$ we require that the range of the functions on the two sides of Eq. (2.28) (as θ varies from 0 to π) be the same (the precise angular dependence of the two sides will be different but this is presumably irrelevant). Using the Poisson summation formula, Eq. (2.20) one finds,[70] for $\Delta\tau \to 0$,

$$e^{-\tilde{K}_x/2} = \frac{K_x}{2} , \tag{2.29}$$

where K_x is given by Eq. (2.15). Inserting Eq. (2.28) into Eq. (2.19) and Fourier transforming[70] one can carry out the $\{\theta\}$ integrations exactly. Their effect is to enforce conservation of integer-valued currents defined by

$$\mathbf{J} = (J^x, J^y, J^\tau) . \tag{2.30}$$

In other words, the current should be divergenceless at every site in space and time; i.e., it should obey a continuity equation

$$\partial_\nu J^\nu = 0 . \tag{2.31}$$

If $J^x_{(x,y,\tau)}$ lies on the bond between sites (x,y,τ) and $(x+1,y,\tau)$, then it is convenient to define $J^{-x}_{(x,y,\tau)} = -J_{(x-1,y,\tau)}$, etc. The divergence constraint is then imposed at each site by requiring that $\sum_\nu J^\nu_{(\mathbf{r},\tau)} = 0$, where ν runs over $\pm x, \pm y, \pm\tau$. We thus obtain

$$Z \approx \sum_{\{\mathbf{J}\}}{}' \exp\left\{ -\frac{1}{2} \sum_{(\mathbf{r},\tau)} \sum_{\nu=x,y,\tau} \tilde{K}_\nu \left(J^\nu_{(\mathbf{r},\tau)} \right)^2 \right\} , \tag{2.32}$$

where the sum is over all integer values of the J^ν from $-\infty$ to ∞, the prime indicates the constraint that $\mathbf{J}$ be everywhere divergenceless, the couplings are

$$\tilde{K}_\tau = U\Delta\tau, \tag{2.33}$$

and $\tilde{K}_y = \tilde{K}_x$ given by Eq. (2.29). Note that in taking the quantum limit, $\Delta\tau \to 0$, the spatial couplings $\tilde{K}_x$ and $\tilde{K}_y$ diverge, while the coupling in the time direction, $\tilde{K}_\tau$, tends to zero. This is the opposite of what we found in the phase representation; see Eqs. (2.15) and (2.22).

We interpret J^ν as the "relativistic" three-vector current with (J^x, J^y) being the spatial current and J^τ being the particle density. Consider the divergenceless current configuration represented by the closed loop in the x-τ plane shown in Fig. 2. The physical interpretation of this is that at time τ_1 a boson hops from position x_1 to position x_2 creating an instantaneous burst of spatial current. This represents a tunneling event in which we assume the barrier is high enough that the tunneling time is small compared to the separation between time slices in our lattice and hence the event can be treated as instantaneous. This approximation affects the ultraviolet

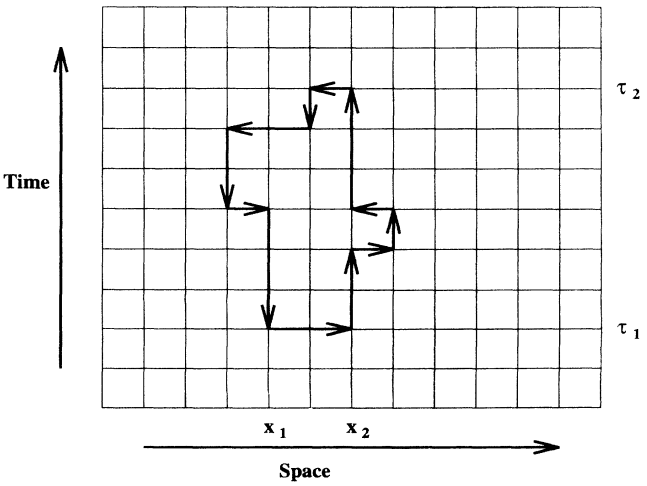

FIG. 2. Typical closed loop of integer-value currents on the links of the space-time lattice. A particle hops from x_1 to x_2 at time τ_1, diffuses until time τ_2 when it annihilates the hole it left behind.

details of the calculation but is irrelevant to the universal zero-frequency behavior. The two vertical lines represent timelike components of the current indicating that there is now a missing boson at x_1 and an excess of one boson at x_2. After some additional random motion, a boson hops back to the original site, leaving the system in the vacuum state at time τ_2.

Notice that for this special case of particle-hole symmetry, the action cost is independent of the sign of J^τ. Recall also that the fact that any integer value of J^τ is allowed (including large negative ones) is due to the fact that J^τ represents the *deviation* of the boson number from its mean value (which is taken to be large and positive).

Our interpretation of the current is confirmed by consideration of the effect of an external vector potential which modifies the potential energy of the quantum rotors to

$$V = -t \sum_{(\mathbf{r},\tau)} \sum_{\nu=x,y} \cos\left(\theta_{(\mathbf{r},\tau)} - \theta_{(\mathbf{r}+\nu,\tau)} + A^\nu_{\mathbf{r}}\right) , \quad (2.34)$$

where $A^\nu_{\mathbf{r}}$ stands for the line integral of the vector potential along the link from site $\mathbf{r}$ to its neighbor in the νth direction. Making this substitution modifies Eq. (2.32) with the result

$$Z \approx \sum_{\{\mathbf{J}\}}{}' \exp\left\{ - \sum_{(\mathbf{r},\tau)} \left[\sum_{\nu=x,y,\tau} \frac{\tilde{K}_\nu}{2} \left(J^\nu_{(\mathbf{r},\tau)}\right)^2 + i \sum_{\nu=x,y} J^\nu_{(\mathbf{r},\tau)} A^\nu_{(\mathbf{r},\tau)} \right] \right\} . \quad (2.35)$$

We note that

$$\left\langle J^\nu_{(\mathbf{r},\tau)} \right\rangle = -i \frac{\delta \ln Z}{\delta A^\nu_{(\mathbf{r},\tau)}} , \ \nu = x, y , \quad (2.36)$$

which means that $J^\nu_{\mathbf{r}}$ must thus be the full, physical, gauge-invariant current, not simply the paramagnetic piece of the current.

From our interpretation that J^τ is the particle density it is now straightforward to include both disorder and a value of the chemical potential which gives a noninteger density, and one finds (see the Appendix for details)

$$Z = \sum_{\mathbf{J}}{}' \exp\left\{ - \sum_{(\mathbf{r},\tau)} \left[\sum_{\nu=x,y,\tau} \frac{\tilde{K}_\nu}{2} \left(J^\nu_{(\mathbf{r},\tau)}\right)^2 - \Delta\tau(\mu + v_{\mathbf{r}}) J^\tau_{(\mathbf{r},\tau)} \right] \right\} . \quad (2.37)$$

We now assume, as in Eq. (2.23), that the universality class is unchanged if we make the couplings isotropic, i.e.,

$$Z = \sum_{\mathbf{J}}{}' \exp\left\{ -\frac{1}{K} \sum_{(\mathbf{r},\tau)} \left[\frac{1}{2} \mathbf{J}^2_{(\mathbf{r},\tau)} - (\tilde{\mu} + \tilde{v}_{\mathbf{r}}) J^\tau_{(\mathbf{r},\tau)} \right] \right\} , \quad (2.38)$$

where we have used Eq. (2.33),

$$\tilde{\mu} = \frac{\mu}{U} , \qquad \tilde{v}_{\mathbf{r}} = \frac{v_{\mathbf{r}}}{U} , \quad (2.39)$$

and K is a dimensionless coupling constant which has to be adjusted to bring the system to the critical point. Varying K corresponds to changing the ratio t/U in the boson Hubbard model, Eq. (2.2), keeping μ/U and Δ/U fixed. Noting the invariance of the action under

$$J^\tau \longrightarrow J^\tau + 1, \qquad \tilde{\mu} + \tilde{v} \longrightarrow \tilde{\mu} + \tilde{v} + 1 , \quad (2.40)$$

we take for simplicity the "largest possible" disorder by choosing $\tilde{\mu} = 1/2, \tilde{\Delta} \equiv \Delta/U = 1/2$. The average particle density is then $1/2$. Note that this choice of parameters has a statistical particle-hole symmetry[71] since, *upon ensemble averaging*, the Hamiltonian is invariant under the transformation $J^\tau \to -J^\tau$, although the presence of the random potential destroys microscopic particle-hole symmetry. We have argued above that lack of *microscopic* particle-hole symmetry[71] changes the universality class from that of the (2+1)D XY model, and so one can ask whether having *statistical* particle-hole symmetry changes the universality class from that of the generic Bose glass to superfluid transition. At least in one dimension, the answer is no, as shown by Fisher,[72] and we shall assume that the same is true in $d = 2$.

We have thus arrived at a representation of the original quantum problem, involving integer link variables. Noting that the J^τ represent the boson density, it can be thought of as an imaginary time "world-line" path-integral representation of the problem, simplified to the extent that it treats just the phase fluctuations of the underlying Hamiltonian.

The partition function, Eq. (2.38) can be written in terms of an effective (2+1)D classical Hamiltonian or action, given by

$$H_V = \frac{1}{K} \sum_{(\mathbf{r},\tau)} \left[\frac{1}{2} \mathbf{J}^2_{(\mathbf{r},\tau)} - (\tilde{\mu} + \tilde{v}_{\mathbf{r}}) J^\tau_{(\mathbf{r},\tau)} \right] . \quad (2.41)$$

Evidently, when $\tilde{v}_{\mathbf{r}} = 0$, integer values of $\tilde{\mu}$ can be absorbed into the definition of $J^\tau_{(\mathbf{r},\tau)}$, and so the model reduces to the (2+1)D Villain model, which is in the same universality class as the (2+1)D XY model. These points are, however, just special multicritical points and the generic behavior is *not* that of the XY model.[10]

We have already noted that the time component, $J^\tau_{(\mathbf{r},\tau)}$, of the link variables corresponds to the particle density or boson occupation number. Long-range Coulomb forces can then be introduced in the following way:

$$H = H_V + H_C , \quad (2.42)$$

$$H_C = \frac{e^{*2}}{K} \sum_\tau \sum_{\langle \mathbf{r},\mathbf{r}' \rangle} (J^\tau_{(\mathbf{r},\tau)} - n_0) G(\mathbf{r} - \mathbf{r}') \times (J^\tau_{(\mathbf{r}',\tau)} - n_0) . \quad (2.43)$$

Here e^* is the effective boson charge, n_0, which repre-

sents the compensating background charge, is the average particle density, and G is the Coulomb interaction. In our simulations with long-range interactions, the particle number was always kept constant, as opposed to the case where only short-range interactions were present where we always allowed the particle number to fluctuate. Calculations of the Coulomb interaction, $G(\mathbf{r})$ must allow for the finite lattice size and periodic boundary conditions. We do this by the usual Ewald method.[73,74] Another way is by a lattice Green's function

$$G(\mathbf{r}) = \frac{2\pi}{L^2} \sum_{\mathbf{k}\neq 0} \frac{\cos(\mathbf{k}\cdot\mathbf{r})}{[4 - 2\cos(k_x) - 2\cos(k_y)]^{1/2}} , \quad (2.44)$$

where $\mathbf{k} = (2\pi/L)(n_x, n_y)$, with $n_x, n_y = 0, \ldots, L-1$. The term with $\mathbf{k} = 0$ is removed to ensure charge neutrality. For large distances and large lattices the Ewald sum and the lattice Green's function become almost identical and approach $1/r$. However, close to the origin the two forms are somewhat different. If the critical properties are universal, they should not depend on the specific form of the potential close to the origin. We use this as a test of our computer codes and of the universality of our results. Indeed as we shall see the two forms yield equivalent results.

III. SCALING THEORY

In order to better understand the universal features of the phase transition it is very useful to consider the scaling behavior of various physical quantities in the regime of the diverging correlation length. Such considerations not only tell us why the conductivity is universal but will tell us how to analyze experimental and Monte Carlo data to determine that one is actually in the critical (scaling) regime.

From now on, we shall denote the number of time slices by L_τ, rather than M, and so the space-time lattice is of size $L \times L \times L_\tau$. Periodic boundary conditions will be applied. Note that the ground state *energy* density of the original 2D quantum problem is related to the *free energy* density of the (2+1)D equivalent classical problem since

$$f = -\lim_{T\to 0} \frac{k_B T}{(aL)^2} \ln Z = -\frac{\hbar}{V} \ln \mathrm{Tr} e^{-H} , \quad (3.1)$$

where H is given by Eq. (2.42), $V = (aL)^2 L_\tau \Delta\tau\hbar$ is the "volume" of the (2+1)D space-time system, with a the lattice spacing in the spatial directions, and $\hbar\Delta\tau$ the lattice spacing in the (imaginary) time direction.

Since space and time are not equivalent, we have two correlation "lengths," ξ in the space direction and ξ_τ in the time direction. These two correlation lengths will diverge with different exponents at the critical point and we can define the dynamical exponent, z, through the relation

$$\xi \sim \delta^{-\nu}, \quad \xi_\tau \sim \xi^z , \quad (3.2)$$

where δ measures the distance from the critical point, K_c, i.e., $\delta = (K - K_c)/K_c$. There is a microscopic frequency, ω_c, related to the lattice spacing $\hbar\Delta\tau$, in the time direction by $\omega_c = 2\pi/(\hbar\Delta\tau)$, and so we can relate ξ_τ more precisely to ξ as

$$\xi_\tau = \frac{1}{\omega_c} \left(\frac{\xi}{b}\right)^z , \quad (3.3)$$

where b is a microscopic length of order the lattice spacing, a.

A. Stiffness

First we discuss the scaling theory describing the singular behavior of the free energy density near the critical point. From Eq. (3.1) one sees that $f/\hbar$ has dimensions of inverse (length^d $\times$ time). Hyperscaling[75] states that multiplying the singular part of this free energy density, f_s, by the (2+1)D correlation volume, $\xi^d\xi_\tau$, one obtains a constant, A, say, of order unity as the critical point is approached, i.e.,

$$\frac{f_s}{\hbar} \xi^d \xi_\tau = A . \quad (3.4)$$

In this section, we will frequently give results for arbitrary space dimension, d, even though we are ultimately interested in the case of $d = 2$. One can consider A to be a critical amplitude for a *dimensionless* quantity (or combination of quantities) which is finite at criticality. According to two-scale factor universality,[76–80] such quantities are not only constants, but are also *universal.*

We next discuss the scaling of the extra free energy cost to impose a twist on the phase of the condensate. We will use this to locate the critical point, K_c, to high accuracy. The extra free energy density is related to the superfluid stiffness, also called the helicity modulus,[81] which is proportional to the superfluid density of the system. A uniform twist in the phase of the order parameter can be introduced by applying a twist of size Θ at the boundary, in (say) the x direction. This will then give rise to a phase gradient

$$\nabla\theta = \Theta/(aL) . \quad (3.5)$$

The (zero-frequency) stiffness, ρ, is then defined by[81,82,54]

$$\frac{\delta f_s}{\hbar} = \frac{1}{2}\rho(\nabla\theta)^2 , \quad (3.6)$$

and so

$$\rho = \frac{(aL)^2}{\hbar} \frac{\partial^2 f_s}{\partial\Theta^2} . \quad (3.7)$$

Since Θ is dimensionless, ρ has dimensions of inverse (length^{d-2} $\times$ time). Hence using hyperscaling and two-scale factor universality we obtain

$$\rho\xi^{d-2}\xi_\tau = C , \quad (3.8)$$

where C is another universal constant. Consequently,

$$\rho \sim \xi^{-(d+z-2)} , \quad (3.9)$$

which is a generalization of the Josephson scaling relation for the classical transition, $\rho_s \equiv (m/\hbar)^2\hbar\rho \sim \xi^{-(d-2)}$. The difference is that d is replaced by $d+z$ for the quantum transition. This replacement also holds for other hyperscaling relations (i.e., those scaling relations involving the space dimensionality).

B. Conductivity

We can extend the notion of a superfluid stiffness, ρ, to a frequency-dependent stiffness, $\rho(i\omega_n)$, where $\omega_n = 2\pi n k_B T/\hbar$ is the Matsubara frequency. The conductivity is then related to $\rho(i\omega_n)$ by the Kubo formula[54]

$$\sigma(i\omega_n) = 2\pi G_Q \frac{\rho(i\omega_n)}{\omega_n} , \tag{3.10}$$

where $G_Q = R_Q^{-1}$, with R_Q defined in Eq. (1.1), is the quantum of conductance. The quantity ρ defined in the previous section is given by $\rho \equiv \rho(0)$. We emphasize that ρ is the stiffness and not the resistivity. Close to the critical point we can generalize Eq. (3.8) to finite frequency[6] by the following scaling assumption:

$$\rho(i\omega_n) = \xi^{2-d}\xi_\tau^{-1}\tilde{\rho}(\omega\xi_\tau) . \tag{3.11}$$

Since the argument of the scaling function $\tilde{\rho}$ is dimensionless, and so has no nonuniversal metric factors associated with it, the *entire scaling function* $\tilde{\rho}(x)$ is universal. Clearly, $\tilde{\rho}(0) = C$, the same universal constant that appears in Eq. (3.8). Furthermore, since $\rho(i\omega_n)$ is finite at finite frequency even at the critical point, one must have, for large x, the asymptotic behavior

$$\tilde{\rho}(x) = D x^{(d+z-2)/z} , \tag{3.12}$$

where D is again universal, in order that the dependence on ξ and ξ_τ cancels at criticality. Substituting this into Eq. (3.10) and noting Eq. (3.3), one has, at criticality,

$$\sigma^* \equiv \lim_{\omega_n \to 0} \sigma(i\omega_n) = 2\pi D\, \sigma_Q\, b^{2-d} \left(\frac{\omega}{\omega_c}\right)^{(d-2)/z} . \tag{3.13}$$

Immediately we see that when $d = 2$ all microscopic lengths and frequencies drop out, and so the dc conductivity is universal[6] at the critical point, given only by fundamental constants and the universal dimensionless number D. The universality of the dc conductivity is analogous to the universal jump[83] in $(\hbar/m)^2\rho_s/k_B T_c$ at the finite-temperature Kosterlitz transition.[5] In fact this quantity corresponds, essentially, to Eq. (3.10) with $\hbar\omega_n$ replaced by $k_B T_c$.

Strictly speaking Eq. (3.13) only refers to the singular part of the conductivity. However, since we approach an insulating phase where the conductivity must be zero, the conductivity cannot have an analytic part at the critical point.

C. Compressibility

The compressibility, κ, is defined by

$$\kappa = \frac{\partial n}{\partial \mu} = \frac{\partial^2 f}{\partial \mu^2} , \tag{3.14}$$

where n is the boson density and μ the chemical potential. We can write an expression equivalent to Eq. (3.6) for the compressibility by noting[10] that the Josephson relation (for imaginary time) is $\delta\mu = \partial\theta/\partial\tau$, and so

$$\delta f = \frac{1}{2}\kappa(\partial_\tau\theta)^2 ; \tag{3.15}$$

i.e., we apply a twist in the (imaginary) time direction instead of along one of the space directions. Note that it is the *total* compressibility which enters this expression.[10] Following the arguments that led to Eqs. (3.8) and (3.9) one finds

$$\frac{\kappa}{\hbar}\xi^d\xi_\tau^{-1} \equiv \frac{\kappa}{\hbar}\xi^d\omega_c\left(\frac{b}{\xi}\right)^z = \text{const}, \tag{3.16}$$

and so

$$\kappa \sim \xi^{-(d-z)} . \tag{3.17}$$

Fisher *et al.*[10] have argued that $z = d$ at the Bose glass to superfluid transition and so the compressibility is finite at criticality. We shall see that our numerical results support this. Note that even in this case, the compressibility is nonuniversal at criticality, because the nonuniversal factors b and ω_c appear in Eq. (3.16). One can also determine the form of the wave-vector-dependent compressibility at criticality, following the scaling arguments that we used above to determine the conductivity. One finds

$$\kappa(k) \sim k^{d-z} . \tag{3.18}$$

IV. QUANTITIES OF INTEREST AND FINITE-SIZE SCALING

In this section we show how to calculate the quantities of interest from the Monte Carlo simulations, and we discuss the finite-size scaling techniques which we will need. Having demonstrated in the last section that the lattice spacings, a and $\hbar\Delta\tau$, do not enter expressions for universal quantities, such as the conductivity at the critical point, we set these lattice spacings (and $\hbar$) to unity from now on.

To perform the quenched disorder averages it is necessary to first do a "thermal" average over the J^ν variables, denoted by $\langle\cdots\rangle$, for a fixed realization of the quenched disorder potential, and then average observables over the quenched disorder $v_{\mathbf{r}}$, which we indicate by $[\cdots]_{\mathrm{av}}$.

A. Stiffness

To calculate the uniform stiffness, $\rho(0)$, note from Eq. (2.34) that a uniform twist in the x direction becomes equivalent to considering the system in the presence of an external vector potential of the form

$$A_{\mathbf{r}}^x = \partial_x\theta\,\delta_{x,\nu} . \tag{4.1}$$

From Eqs. (2.34), (3.7), and (4.1) one finds that

$$\rho(0) = \frac{1}{L^d L_\tau}\left[\left\langle\left(\sum_{(\mathbf{r},\tau)} J^x_{(\mathbf{r},\tau)}\right)^2\right\rangle\right]_{\rm av} . \tag{4.2}$$

Near the critical point, the correlation length is much larger than the size of the system, and so finite-size effects will be important. We therefore need to derive a finite-size scaling form[84] for the stiffness. The basic finite-size scaling hypothesis is that the size of the system only appears in the ratio L/ξ, and, for quantum problems, the corresponding ratio in the time direction, L_τ/ξ_τ. Thus we have

$$\rho(0) = \xi^{-(d+z-2)} P(L/\xi,\ L_\tau/\xi_\tau) , \tag{4.3}$$

which can be more conveniently expressed as

$$\rho(0) = \frac{1}{L^{d+z-2}}\bar{\rho}\left(L^{1/\nu}\delta,\ \frac{L_\tau}{L^z}\right) , \tag{4.4}$$

where P and $\bar{\rho}$ are scaling functions. It is thus essential to work with system shapes for which the aspect ratio

$$c = L_\tau/L^z \tag{4.5}$$

is a constant; otherwise the scaling function $\bar{\rho}$ depends on two variables and is complicated to analyze. If this is done, $L^{d+z-2}\rho$ is *independent* of L at the critical point $\delta = 0$. Furthermore, in the disordered state, the system is insensitive to changes in the boundary conditions if the size is bigger than the correlation length, and so $L^{d+z-2}\rho$ will *decrease* (exponentially) with increasing L. By contrast, in the ordered state, ρ tends to a constant, and so $L^{d+z-2}\rho$ *increases* with increasing L. Thus, the critical point is located at the intersection of curves for $L^{d+z-2}\rho$ as a function of coupling K for different lattice sizes. One can then determine ν from Eq. (4.4) by requiring that the data for different sizes (but fixed aspect ratio) collapse on top of each other in a plot of $\rho(0)L^{d+z-2}$ against $L^{1/\nu}\delta$. Note that in order to choose the sample shapes in the simulation, we need (unfortunately) to have already made a choice for z.

Since the current is divergenceless, we can divide the configurations into different topological classes according to the winding number of the boson world lines around the torus of size L in the space direction

$$n_x \equiv L^{-1}\sum_{(\mathbf{r},\tau)} J^x_{(\mathbf{r},\tau)} , \tag{4.6}$$

so that the stiffness is simply proportional to the mean-square winding number

$$\rho(0) = \frac{1}{L_\tau}\left[\langle n_x^2\rangle\right]_{\rm av} . \tag{4.7}$$

It is instructive to comment on the analogy to the Feynman ring exchange picture of superfluidity in liquid helium.[85] Rather than viewing a nonzero winding of a boson world line as an event involving a single boson, we can view it as formed by adding up a chain of hops of many bosons. This is closely analogous to a Feynman ring exchange, and adds some perspective on the transition in our model. The superfluid stiffness arises due to macroscopic condensation of ring exchanges of global currents carrying nonzero winding number, and the critical point is where the gain in free energy from the "entropy" of the ring exchanges matches their energy cost. In the presence of macroscopic ring exchanges which wind around the sample, the free energy is sensitive to Aharonov-Bohm flux (boundary condition twists) and hence the system exhibits off-diagonal long-range order in the conjugate phase variable.

B. Conductivity

The frequency-dependent stiffness involves the Fourier transform of the current-current correlation function

$$\rho(i\omega_n) = \frac{1}{L^2 L_\tau}\left[\left\langle\left|\sum_{(\mathbf{r},\tau)} e^{i\omega_n\tau} J^x_{(\mathbf{r},\tau)}\right|^2\right\rangle\right]_{\rm av} , \tag{4.8}$$

where, with the lattice spacings in the space and time directions set to unity, the Matsubara frequency is given by $\omega_n = 2\pi n/L_\tau$, and τ is now an *integer*, $1 \le \tau \le L_\tau$, denoting a particular time slice. In these units, the conductivity is still given by Eq. (3.10).

C. Compressibility

From Eq. (3.14) it follows that the zero wave-vector compressibility is given by

$$\kappa(0) = \frac{1}{L^2 L_\tau}[\langle N_b^2\rangle - \langle N_b\rangle^2]_{\rm av} , \tag{4.9}$$

where N_b is the total number of particles,

$$N_b = \frac{1}{L_\tau}\sum_{(\mathbf{r},\tau)} J^\tau_{(\mathbf{r},\tau)} . \tag{4.10}$$

The last term in Eq. (4.9) involves the square of a thermal average. This term is thus likely to give systematic errors[86] if determined within one replica, and so we evaluate it as $[\langle N_\alpha\rangle\langle N_\beta\rangle]_{\rm av}$, where the indices refer to two different replicas.

If global moves are not included, the boson density is a constant, and consequently κ, as defined, is zero. However, the wave-vector-dependent compressibility $\kappa(k)$ is nonzero, and one can obtain[49] estimates of $\kappa = \kappa(0)$ by taking the limit $k \to 0$, even when global moves are not performed.

The finite-size scaling form for the compressibility follows from arguments similar to those used above for the stiffness and is

$$\kappa = \frac{1}{L^{d-z}}\tilde{\kappa}\left(L^{1/\nu}\delta,\ \frac{L_\tau}{L^z}\right) . \tag{4.11}$$

D. Correlation functions

Consider the following correlation function

$$C(\mathbf{r},\mathbf{r}',\tau,\tau') = [\langle e^{i[\hat{\theta}_{\mathbf{r}}(\tau)-\hat{\theta}_{\mathbf{r}'}(\tau')]}\rangle]_{\rm av} , \tag{4.12}$$

where the $\hat{\theta}$'s are operators for the phase of the bosons, and $e^{i\hat{\theta}_{\mathbf{r}}(\tau)} = e^{\tau H} e^{i\hat{\theta}_{\mathbf{r}}} e^{-\tau H}$. We shall see that this correlation function gives information on a third critical exponent, η, defined in Eq. (4.18) below, in addition to the exponents ν and z already discussed. Due to translational invariance, $C(\mathbf{r},\mathbf{r}',\tau,\tau') = C(\mathbf{r}-\mathbf{r}',\tau-\tau')$.

We shall here only consider two basic types of correlations: the equal-time correlation function where $\tau = 0, \mathbf{r} = (x,0)$, and the time-dependent correlation function at time τ and $\mathbf{r} = 0$. By redoing the argument which led from Eqs. (2.4) to (2.32) for the correlation function rather than for the partition function, one finds that the equal-time correlation function can be expressed as

$$C_x(r) = \left[\left\langle \prod_{\mathbf{r} \in \text{path}} \exp\left\{ -\frac{1}{K}\left(J^{\nu}_{(\mathbf{r},\tau)} + \frac{1}{2} \right) \right\} \right\rangle \right]_{\text{av}} , \tag{4.13}$$

where "path" is any path on the lattice at fixed τ connecting two points a distance r apart along the x direction. For each link on the path $\nu = x$ or y, depending on whether the link is along the x or y direction. The simplest case, which was used in the simulations, is the straight line path, in which case all the link variables in Eq. (4.13) are J^x. A very similar result is found for the usual Villain model.[70] Since the Hamiltonian is invariant under a sign change of J_x, it follows that $C_x(r) = C_x(-r)$.

We now turn to the time-dependent correlation function

$$C_+(\tau) \equiv C(\mathbf{r}=0,\tau) = [\langle e^{i(\hat{\theta}_{\mathbf{r}}(\tau) - \hat{\theta}_{\mathbf{r}}(0))} \rangle]_{\text{av}} . \tag{4.14}$$

Physically this is the Green's function for creating a particle at imaginary time 0 and destroying it at time τ. This correlation function can be expressed in terms of the link variables in the following form:

$$C_+(\tau) = \left[\left\langle \prod_{\tau \in \text{path}} \exp\left\{ -\frac{1}{K}\left(\frac{1}{2} + J^{\tau}_{(\mathbf{r},\tau)} - \tilde{\mu}_{\mathbf{r}} \right) - \frac{e^{*2}}{K}\left[\sum_{\mathbf{r}}{}' (J^{\tau}_{(\mathbf{r}',\tau)} - n_0) G(\mathbf{r}-\mathbf{r}') + \frac{1}{2L^2}\sum_{\mathbf{r}} [G(0) - G(\mathbf{r})] \right] \right\} \right\rangle \right]_{\text{av}} . \tag{4.15}$$

In this expression, "path" is the straight line path between two points with the same space coordinate, $\mathbf{r}$, starting at imaginary time equal to 0, say, and ending at a later time τ. A more general expression for a path wandering in the space directions can also be derived.

One can also consider

$$C_-(\tau) = [\langle e^{-i[\hat{\theta}_{\mathbf{r}}(\tau) - \hat{\theta}_{\mathbf{r}}(0)]} \rangle]_{\text{av}} , \tag{4.16}$$

which is the Green's function for creating a *hole* at imaginary time 0 and destroying it at τ. In terms of the link variables

$$C_-(\tau) = \left[\left\langle \prod_{\tau \in \text{path}} \exp\left\{ -\frac{1}{K}\left(\frac{1}{2} - J^{\tau}_{(\mathbf{r},\tau)} - \tilde{\mu}_{\mathbf{r}} \right) + \frac{e^{*2}}{K}\left[\sum_{\mathbf{r}}{}' (J^{\tau}_{(\mathbf{r}',\tau)} - n_0) G(\mathbf{r}-\mathbf{r}') - \frac{1}{2L^2}\sum_{\mathbf{r}} [G(0) - G(\mathbf{r})] \right] \right\} \right\rangle \right]_{\text{av}} . \tag{4.17}$$

Except when there is statistical particle-hole symmetry,[71] $C_+(\tau) \neq C_-(\tau)$.[87] However, one can show that $C_+(\tau) = C_-(L_\tau - \tau)$, which corresponds to the equivalence between a particle traveling forwards in time and a hole traveling backwards. This will be useful in the simulation because the statistics get worse with increasing τ, and so, for $\tau > L_\tau/2$, it is better to compute $C_-(L_\tau - \tau)$ than $C_+(\tau)$. As required, the correlation functions are periodic, i.e., $C(\tau) = C(\tau + L_\tau)$ for both C_- and C_+.

Following Ref. 10 we now make the assumption that the long-distance, large-time behavior of the correlation functions will be given by the scaling form

$$C(\mathbf{r},\tau) = r^{-(d+z-2+\eta)} f(r/\xi, \tau/\xi^z) , \tag{4.18}$$

which defines the exponent η. If $\mathbf{r}$ approaches zero but τ remains finite, the correlation functions must remain finite and nonzero. Thus we obtain

$$C(\mathbf{r}=\mathbf{0},\tau) = \tau^{-(d+z-2+\eta)/z} g(\tau/\xi^z) . \tag{4.19}$$

At the critical point we should therefore have

$$\begin{aligned} C_x(r) &\sim r^{-y_x} , \\ C_\tau(\tau) &\sim \tau^{-y_\tau} , \end{aligned} \tag{4.20}$$

where

$$\begin{aligned} y_x &= d + z - 2 + \eta , \\ y_\tau &= (d + z - 2 + \eta)/z . \end{aligned} \tag{4.21}$$

Thus the power law falloff of the correlation functions at criticality determines both η and z provided the correla-

tion functions can be evaluated for large enough system sizes that finite-size corrections are unimportant.

V. MONTE CARLO METHODS

To satisfy the zero divergence criterion in Eq. (2.31) our basic (local) Monte Carlo move consists of changing all the link variables around one plaquette simultaneously in the manner shown in the lower left corner of Fig. 3, thus changing the local current. Two of the link variables are increased by one, the other two decreased by one. An equivalent move going in the other direction is also used; i.e., the plusses and minuses are interchanged. In addition, we need to include nonlocal moves to fully equilibrate the system. The global moves consist of changing by ± 1 a line of link variables stretching all through the system. Nonlocal moves are included in all three directions $\delta = x, y, \tau$, except when the model has long-range interactions, in which case no global moves in the time direction are performed in order to keep the particle number constant. Global moves in the time direction amount to either introducing or destroying a boson. It is easy to see that global moves in the space directions correspond to a change in the winding number,[49,51] defined in Eq. (4.6). The nonlocal moves we use are illustrated in Fig. 3. One Monte Carlo sweep of the lattice consists of a sweep of local moves followed by a sweep of global moves.

Due to the continuity equation, Eq. (2.31), the sum of $J^\tau_{\mathbf{r}}$ at a given time slice, $\sum_{\mathbf{r}} J^\tau_{\mathbf{r}}$, is always the same for

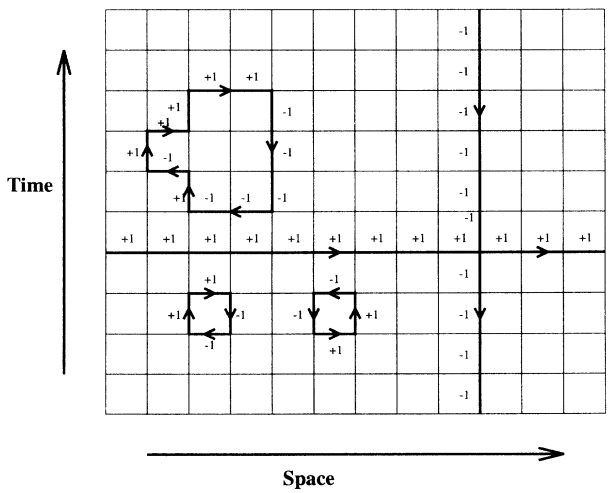

FIG. 3. Schematic picture of a local move (lower left corner), and global move (right side of the picture). In the local moves changes of ± 1 are attempted in the currents circulating around a plaquette. In the global the current is changed by ± 1 along straight lines across the system, thereby changing the winding number, if the line is along a space direction, or the boson number if the line is in the time direction. The numbers indicate how the link variables are changed. Many local moves will change the current around an arbitrary loop as indicated in the upper left corner. A global move which destroys a boson is shown, and also another global move which increases the winding number along the x direction by one.

any value of τ; albeit this constant may vary as a function of Monte Carlo time because of global moves in the time direction. Likewise, the sum of J^x in any y-τ plane will be the same for all such planes at a fixed Monte Carlo time, and similarly for the sum of the J^y.

Expectation values of observables have to be computed by quenched disorder averaging, which is known from the study of spin glasses[88] to have many potential pitfalls. Close to the critical point we typically have to average over from 200 to 1000 different realizations of the disorder, and somewhat fewer away from the critical point. It is crucial to carefully assure that the J^ν variables are thermally equilibrated. The equilibration time at the critical point for our update scheme varies with system size L as $\tau_{\mathrm{MC}} \sim L^{z_{\mathrm{MC}}}$, where z_{MC} is the Monte Carlo dynamic exponent. For the short-range interaction case we have determined[65] $z_{\mathrm{MC}} \approx 6$ so that extreme caution is required in attempting to equilibrate large lattices. We take an approach similar to what has been done for spin glass systems.[86] Two identical replicas are run in parallel for a given realization of the disorder. We define the "Hamming" distance between replicas α and β as

$$h^\nu_{\alpha,\beta}(t) = \sum_{(\mathbf{r},\tau)} \left[J^\nu_{(\mathbf{r},\tau),\alpha}(t_0 + t) - J^\nu_{(\mathbf{r},\tau),\beta}(t_0 + t) \right]^2 , \tag{5.1}$$

where t_0 is the number of Monte Carlo sweeps (MCS) used for equilibration, and t is the number of subsequent MCS. We also define a "Hamming" distance for one replica at two different Monte Carlo times,

$$h^\nu_{\alpha}(t) = \sum_{(\mathbf{r},\tau)} \left[J^\nu_{(\mathbf{r},\tau),\alpha}(t + t_0) - J^\nu_{(\mathbf{r},\tau),\alpha}(t_0) \right]^2 . \tag{5.2}$$

We determine $[h^\nu_{\alpha,\beta}(t_0)]_{\mathrm{av}}$ and $[h^\nu_{\alpha}(t_0)]_{\mathrm{av}}$ for a sequence of values of t_0 increasing exponentially, $t_0 = 10, 30, 100, 300, 1000, \ldots$, up to $t_0 = T_0$, and so T_0 is both the number of MCS for measurement and the number of MCS for equilibration. If t_0 is sufficiently large that the system has equilibrated, one has $[h^\nu_{\alpha,\beta}(t_0)]_{\mathrm{av}} = [h^\nu_{\alpha}(t_0)]_{\mathrm{av}}$, and we made sure that this condition was fulfilled, at least for $t_0 = T_0$. To achieve equilibration we took T_0 to be of order 3000 for the smaller system sizes but found that we needed up to 30 000 for the larger sizes. Since the different disorder realizations give statistically independent thermal averages, we can estimate the statistical error from the standard deviation of the results for different samples. Note that there are big sample to sample fluctuations, and so it is necessary to average over a large number of samples. In order to study as many samples as possible within the available computer time, we only run each sample for the minimum number of MCS necessary to get a few statistically independent measurements. This is why the number of sweeps for averaging is the same as the number used for equilibratior

VI. SHORT-RANGE INTERACTIONS

In this section we shall assume that no long-range Coulomb interactions are present. Furthermore, we shall

always take the random chemical potential to be specified by

$$\tilde{\mu} = \frac{1}{2}, \quad \tilde{\Delta} = \frac{1}{2} . \tag{6.1}$$

The reason for this choice of $\tilde{\mu}$ is that we want to be as far away as possible from any Mott insulator phase,[10] and these are centered on integer values of $\tilde{\mu}$ for weak disorder. The choice of $\tilde{\Delta}$ was influenced by the need to make the disorder not too small (otherwise the effects of disorder would only be seen for large sizes which we are unable to simulate) and also not too large, because this effectively makes U small, and so, again, the asymptotic behavior may only set in for large sizes. In the absence of more detailed information, it seems sensible to make all the important couplings of comparable size. We again emphasize that universal quantities like the critical conductivity are independent of these details.

Some inequalities involving the critical exponents ν, η, and z have been obtained. First of all, Fisher *et al.*[10] have argued that the compressibility is finite at the transition and so

$$z = d . \tag{6.2}$$

Fisher *et al.*[10] also argue that

$$\eta \leq 2 - d , \tag{6.3}$$

on the grounds that the density of states should diverge as the transition is approached from the Bose glass side. In addition, since the correlations must decay with distance at criticality, it follows from Eq. (4.18) that

$$d + z - 2 + \eta > 0 . \tag{6.4}$$

Note that since $z > 0$ one can have a negative η even in two dimensions. There is also a general inequality applicable to random systems,[89,90]

$$\nu \geq \frac{2}{d} , \tag{6.5}$$

which is a generalization of the Harris criterion.[91] The value of the dimension that should be inserted into this expression is the number of dimensions in which the system is random, i.e., the space dimension d and not $d+1$ or $d+z$.

As noted in the discussion below Eq. (4.5) we need to know the dynamical exponent z in order to choose sample shapes which allow a simple finite-size scaling analysis; i.e., the samples should be of size $L \times L \times cL^z$, where c is the aspect ratio. Most of the simulations were done assuming $z = 2$, the value predicted by Fisher *et al.*[10] We have done additional simulations with shapes corresponding to other values of z, but find that the scaling is much less good if z is significantly different from 2. For $z = 2$ we have taken two different aspect ratios 1/2 and 1/4, with the following systems sizes: $4\times4\times8$, $6\times6\times18$, and $8\times8\times32$ for aspect ratio 1/2, and $6\times6\times9$, $8\times8\times16$, and $10 \times 10 \times 25$ for aspect ratio 1/4. We were unable to study larger lattices because the relaxation times were too long.

As a test of our program we checked that we were able to reproduce the results of Ref. 54 in the absence of disorder and with $\tilde{\mu} = 0$. We found complete agreement[58] between the two simulations.

A. Equilibration

We test for equilibration using the method described in Sec. V. As an example, Fig. 4 shows the Hamming distance for the x and τ link variables for a system of size $8 \times 8 \times 16$, at the critical point. We see that the system equilibrates rather quickly in about 1000 MCS. Also, we see that the x and τ link variables equilibrate in roughly the same time, as one would expect since they are coupled through local moves.

B. Determination of the critical point

We start the analysis by locating the critical point. Since, as discussed above, we assume that $z = d = 2$, the relevant quantity to plot, according to the finite-size scaling analysis in Sec. IV A, is $\rho(0)L^2$. Results for aspect ratio 1/4 are shown in Fig. 5. Since the critical point is located where the curves cross, the figure demonstrates clearly that there is a transition close to $K = 0.25$ between a superfluid phase for $K > K_c$ with finite superfluid density, ρ_s [remember that $\rho_s \sim \rho(0)$], and an insulating phase for $K < K_c$ with zero superfluid density. Our best estimate of the critical coupling is $K_c = 0.248 \pm 0.002$. A substantial amount of computation went into the production of this figure. Close to the critical point 1000–2000 disorder realizations were performed, with, for the largest size, an equilibration time of $T_0 = 10\,000$ followed by 10 000 MCS for averaging with a measurement every 10 MCS.

Simulations with aspect ratio 1/2 were also performed and the same critical coupling was found, as expected since this is a bulk property.

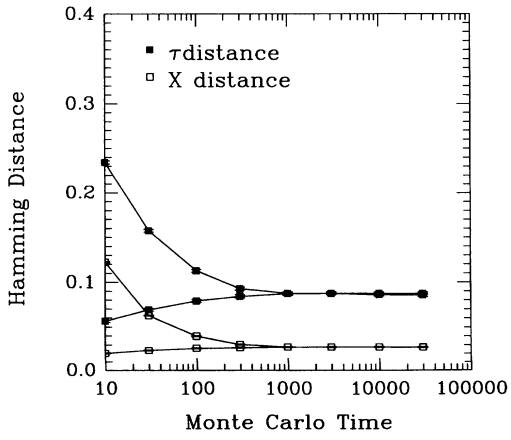

FIG. 4. The x and τ Hamming distances for a system of size $8 \times 8 \times 16$, with short-range interactions at the critical coupling $K = 0.248$. For each pair of curves, the upper one is for $h_{\alpha,\beta}$ and the lower one for h_α.

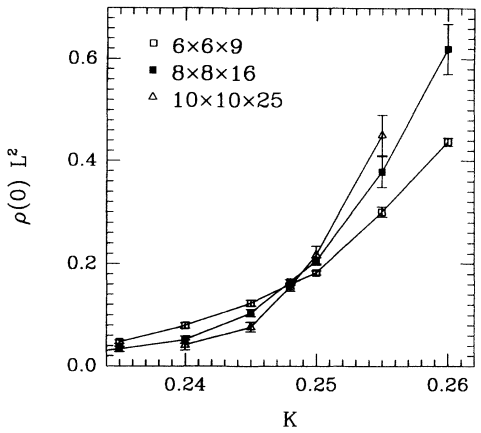

FIG. 5. $\rho(0)L^2$ for the system sizes indicated, as a function of K for short-range interactions. From the intersection of the curves we estimate the critical coupling to be $K_c = 0.248 \pm 0.002$.

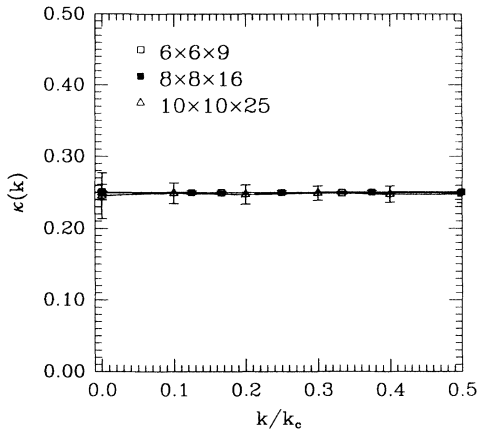

FIG. 7. The compressibility of the model with short-range interactions as a function of wave vector, at the critical point, $K_c = 0.248$, for different system sizes. The solid lines are spline fits to the data points, and $k_c = 2\pi$.

C. Compressibility

We now turn to the compressibility. Figure 6 shows the compressibility, as calculated from Eq. (4.9), for a range of different couplings centered around the critical coupling $K_c = 0.248$, for lattices with aspect ratio 1/4. We see that the compressibility remains finite through the transition, including in the insulating phase, $K < K_c$. This is consistent with the prediction that the insulating phase should be a Bose glass with finite compressibility in the presence of disorder.[10] According to the scaling theory, Eq. (3.17), a finite compressibility at criticality implies $z = d$ (= 2), as argued by Fisher *et al.*[10] By contrast, simulations performed[58] with no disorder and $\tilde{\mu} = 0$, where the model becomes equivalent to a (2+1)D XY model, find that the compressibility vanishes in the insulating phase, consistent with its being a Mott insulator.

Figure 7 shows the wave-vector-dependent compressibility for the aspect ratio 1/4, at the critical point $K_c = 0.248$. Similar results have been obtained for the aspect ratio 1/2. Clearly there is no dependence on the wave vector as expected from Eq. (3.18) and the result $z = d$.

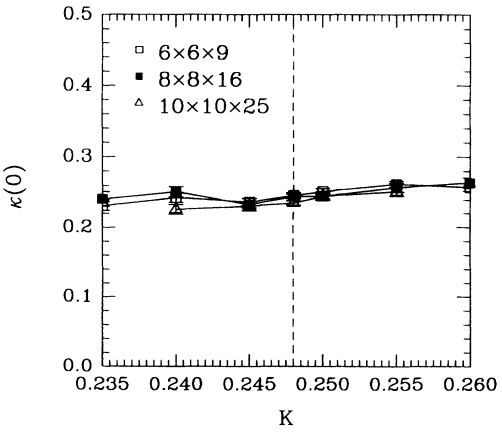

FIG. 6. The compressibility at zero wave vector, $\kappa(0)$, for different system sizes, as a function of K for short-range interactions. The critical point is at $K_c = 0.248$.

From the above we have established that the insulating phase is indeed a Bose glass and not a Mott insulator, at least for the strength of the disorder that we have been considering here, $\Delta = 1/2$. This is in agreement with previous studies.[52,53,43,57]

As further evidence of the existence of the Bose glass we now turn to a discussion of the correlation functions in the insulating phase. One important prediction of the scaling theory[10] is that the Green's function should vary with a power of imaginary time,

$$C(\mathbf{r} = 0, \tau) \sim \rho_1(0)/\tau \ , \tag{6.6}$$

rather than exponentially, as might have been expected. Here $\rho_1(0)$ is the single-particle density of states at zero energy. In order to check this prediction we did simulations deep in the insulating phase, $K < K_c$. Figure 8 shows the time-dependent correlation function, $C_+(\tau) \equiv C(\mathbf{r} = 0, \tau)$, for a system of size $8 \times 8 \times 16$ at a coupling equal to $K = 0.175$, well below $K_c \simeq 0.248$. The right hand part of the figure is obtained by calculating $C_-(\tau)$, and using the relation $C_+(\tau) = C_-(L_\tau - \tau)$ discussed in Sec. IV D. For each disorder realization, 30 000 MCS were performed, followed by another 30 000 MCS to do the thermal averaging, and finally we averaged over 100 different disorder realizations. The relatively elaborate thermal averaging was done in order to obtain small error bars at large τ. The dashed line is a power-law fit to the form $0.170(2)[\tau^{-1.10(8)} + (L_\tau - \tau)^{-1.10(8)}]$ where the numbers in parentheses indicates uncertainties on the last digit. This fit used all data points shown and gave a goodness of fit of 0.84 and $\chi^2 = 7.9$. Here we define the goodness of fit to be $\Gamma((N-2)/2, \chi^2/2)$, where N is the number of data points and Γ is the incomplete γ function. No sign of an exponential dependence on τ was

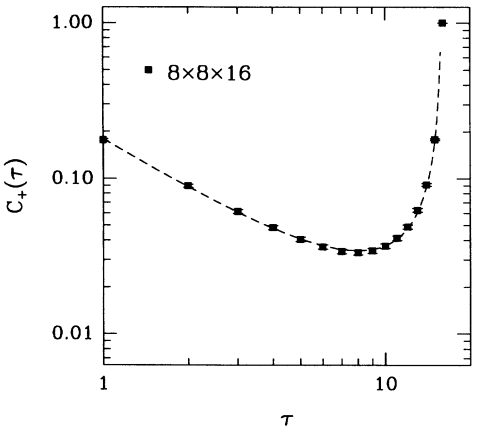

FIG. 8. The correlation function (imaginary time Green's function) for positive (imaginary) times, corresponding to a boson propagating forward in time, for a system of size $8 \times 8 \times 16$ with short-range interactions, at $K = 0.175$ which is far into the Bose glass phase. The dashed line indicates a fit to the data of the form $0.170(2)(\tau^{-1.10(8)} + (L_\tau - \tau)^{-1.10(8)})$. The data for $\tau > L_\tau/2$ are actually the value of $C_-(L_\tau/2 - \tau)$ as discussed in the text. Thus the Green's function decays with a power of time (rather than exponentially) in the Bose glass phase, as predicted in Ref. 10.

observed. The errors indicated are statistical and do not include possible systematic errors. A fit at $K = 0.15$ yielded a similar value for the exponent of 1.05 ± 0.04. We conclude that the time-dependent correlation functions clearly display power-law behavior in the Bose glass phase and, furthermore, the associated exponent is close to 1 as predicted by scaling theory.[10]

D. Conductivity

In the thermodynamic limit, $L \to \infty$, at vanishingly small T ($L_\tau \to \infty$), and for $\omega_n \to 0$, the conductivity at the critical point should tend to a finite, universal value, σ^*, as discussed in Sec. III B. In the simulation there will be various corrections to this. First of all, one might ask whether the order of limits $T \to 0$ and $\omega_n \to 0$ affects the value of σ^*, even in the thermodynamic limit. For the case of no disorder and integer filling, where the transition is to the Mott insulator, the answer is certainly yes.[54] In this case the conductance is finite if the $T \to 0$ limit is taken first whereas $\sigma^* = \infty$ if one first takes the zero-frequency (dc) limit because a persistent current can flow in the absence of umklapp processes, which vanish as $T \to 0$. However, in the presence of disorder, the dc conductivity is finite as $T \to 0$ and so we see no reason why the order of the limits, $T \to 0$ and $\omega_n \to 0$ should play a role for transition to the Bose glass phase discussed here. We shall see that allowing for a dependence on $\omega_n/T \propto \omega_n L_\tau$ does give a slighly better fit for the case of short-range interactions, but the value of σ^* is not changed significantly. Given the rather limited range of sizes that we can study, we feel that the results are consistent with there being *no* dependence on ω_n/T. One might also be concerned about finite-size corrections to the conductivity, but our results are consistent with their being very small. Of course, the conductivity is frequency dependent and so will differ from the universal value when ω_n becomes comparable with some other scale, such as the ultraviolet cutoff set by the lattice spacing.

Figure 9 shows the resistance per square (which is the same as the resistivity) plotted against frequency,[92] evaluated from Eq. (3.10) for aspect ratio 1/4 at the critical point $K_c = 0.248$. Again considerable computation has gone into the production of this graph in order to obtain good statistics. For the two smallest system sizes about 2000 disorder configurations were generated while for the largest size only 1000 were done. From 3000 to 10 000 MCS were done for equilibration followed by the same number of sweeps for measurements. The data collapse is excellent.

To determine the universal conductivity we have to analytically continue the MC data to real frequency and extrapolate to $\omega = 0$. For typical quantum MC simulations, this analytic continuation is extremely difficult to perform. However, it turns out to be straightforward in the present case, since the data for the resistivity varies linearly at small ω_n, which implies

$$\sigma(i\omega_n) = \frac{\sigma^*}{(1 + |\omega_n|\tau_0)} \,. \tag{6.7}$$

This is easily seen to analytically continue to the Drude form of the conductivity:

$$\sigma(\omega + i\delta) = \frac{\sigma^*}{(1 - i\omega\tau_0)} \,. \tag{6.8}$$

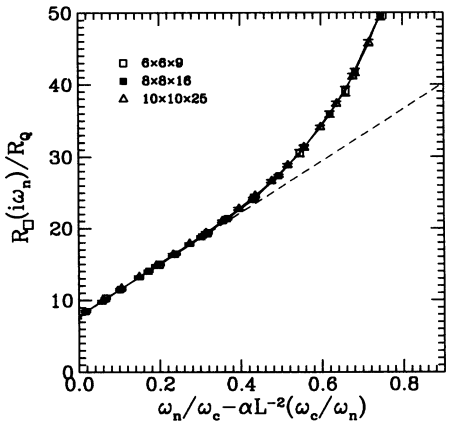

FIG. 9. The resistivity in units of $R_Q = h/(2e)^2$, as a function of $\omega_n/\omega_c - \alpha L^{-2}(\omega_c/\omega_n)$ for the model with short-range interactions, where $\omega_c = 2\pi$ and $\alpha = 0.179$. The calculation was done at the critical point, $K = 0.248$. The aspect ratio was in this case 1/4, and the system sizes shown were as indicated in the figure. The dashed line indicates a least square fit to the points with abscissa less than 0.26 of the following form $7.84(7) + 34.9(5)[\omega_n/\omega_c - \alpha L^{-2}(\omega_c/\omega_n)]$. The correction involving the parameter α is proportional to T/ω_n as discussed in the text. On physical grounds we expect that $\alpha = 0$ in the thermodynamic limit, and indeed a fairly good fit, with almost the same value of the dc resistivity, is obtained with $\alpha = 0$.

Thus the boson system at the critical point is neither insulator nor superfluid but rather a Drude metal. The Drude parameter $\tau_0 \sim 1/\omega_c$ is a nonuniversal relaxation time controlled in our model by the ultraviolet cutoff.

Assuming this linear variation of the resistivity with ω_n, a least squares fit has a very small error. The main source of error in the determination of the dc conductivity therefore comes from the uncertainty in the determination of the critical point. We estimated this error by making the same linear fit to the resistivity data at the ends of the interval given by the error bars of the critical coupling. From all our data for two different aspect ratios we finally estimate

$$\sigma^* = (0.14 \pm 0.03) G_Q \ , \quad R^*_\square = (7.4 \pm 1.6) R_Q \ . \tag{6.9}$$

The universal conductivity has previously been calculated for the case of no disorder and integer boson filling,[54] where the insulating phase is a Mott insulator, rather than the Bose glass discussed here. In that case $\sigma^* \simeq 0.285 G_Q$. Thus we find that even though the present model is somewhat more realistic, including the disorder takes us *further* from the experimental value which is in the vicinity of unity. A suitably defined universal conductance can be calculated exactly in 1D (Ref. 54) both with and without disorder. The exact solution in 1D shows that the ratio of σ^* in the dirty case and in the pure case is exactly 3/4. This is of the same order of magnitude as the ratio $0.14/0.285 \simeq 0.5$ between the MC results in 2D. Hence we see that the trend of decreasing critical conductivity upon adding disorder is the same as for the exact solution in 1D.

E. Exponent ν

To determine the correlation length exponent we try to collapse the data in a scaling plot of $\rho(0)L^2$ versus $\delta L^{1/\nu}$, based on Eq. (4.4). The plot is shown in Fig. 10, for which the parameters used are $K_c = 0.248$ and $\nu = 0.9$. From this and other plots for different values of the aspect ratio we estimate

$$\nu = 0.90 \pm 0.10 \ . \tag{6.10}$$

Interestingly, the inequality, $\nu \geq 2/d$ (with $d = 2$ here) derived by Chayes *et al.*[89] is only just satisfied and may, in fact, be an equality for this model. The equality, $\nu = 2/d$, has been found for certain models of correlated disorder.[93]

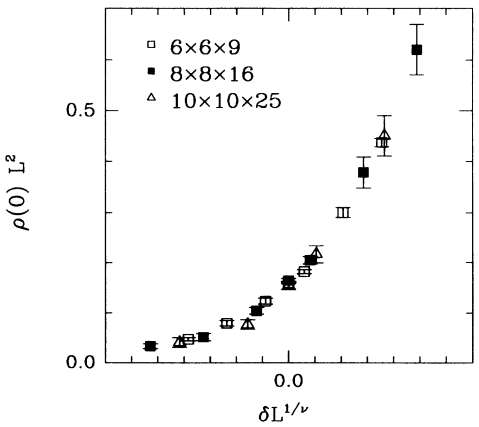

FIG. 10. Scaling plot of $\rho(0)L^2$ versus $\delta L^{1/\nu}$, for short-range interactions, where δ is the reduced coupling constant $(K - K_c)/K_c$ and L is the linear system size. The parameters used in the plot are $K_c = 0.248$, $\nu = 0.90$.

F. Correlation functions

So far, we have determined the universal values of ν and σ^*. We have also found that the finite-size scaling works best with $z = 2$ and, according to the scaling theory, our results for the compressibility agree with this. In this subsection we conclude our discussion of the model with short-range interactions by looking at the correlation functions, which give us the value of the third exponent, η, and another estimate for z.

The data for $C_x(r)$ for sizes $L = 8$ and 10 with aspect ratio 1/4 at $K_c = 0.248$ are shown in Fig. 11. In order to make full use of all the points we fit the correlation functions to the following form:

$$C_x(r) = c[r^{-y_x} + (L - r)^{-y_x}] \ , \tag{6.11}$$

which takes the periodic boundary conditions into account. For $L = 8$ the best fit had the form $0.18(1)(r^{-2.02(1)} + (L - r)^{-2.02(1)})$. For $L = 10$ the fit was $0.18(1)(r^{-1.94(2)} + (L - r)^{-1.94(2)})$. These fits are

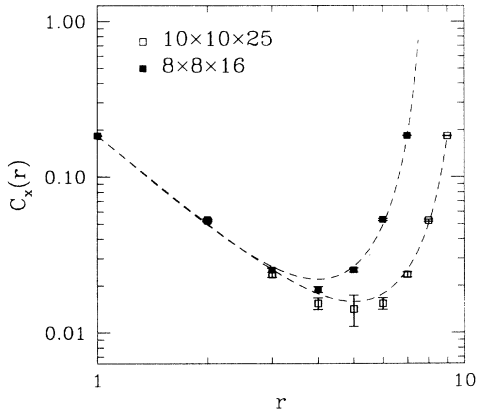

FIG. 11. The equal-time correlation function of the x-link variables as a function of spatial distance $r(= x)$ for short-range interactions. The error bars increase with increasing r because the calculation involves the average of the exponential of a "string" of link variables [see Eq. (4.13)], which can fluctuate hugely when the string is long. For this reason, the data for $r > L/2$ were determined from $C_x(L - r)$. Two data sets are shown, for systems of size $L = 8$ and 10 with aspect ratio 1/4, at $K = 0.248$, which is the critical point. The dashed line indicates fits to the data. For $L = 8$ the fit is $0.18(1)(r^{-2.02(1)} + (L - r)^{-2.02(1)})$. For $L = 10$ the fit is $0.18(1)(r^{-1.94(2)} + (L - r)^{-1.94(2)})$.

indicated by the dashed lines in Fig. 11.

In order to obtain η and z from Eq. (4.21) we also need to obtain results for the time-dependent correlations. Since $\tilde{\mu} = 0.5$ there is statistical particle-hole symmetry[71] and so $C_-(\tau) = C_+(\tau)$. Figure 12 shows the results at the critical point $K_c = 0.248$ for an aspect ratio of 1/4, where the data for $\tau \geq L_\tau/2$ were obtained from $C_-(L_\tau - \tau)$. The linear sizes were $L = 6$ and 8. We fit to the form

$$c[\tau^{-y_\tau} + (L_\tau - \tau)^{-y_\tau}] , \tag{6.12}$$

and we find for $L = 6$ the optimal fit has the form $0.266(4)(\tau^{-1.03(1)} + (L-\tau)^{-1.03(1)})$. For $L = 8$ the best fit has the form $0.256(4)(\tau^{-0.94(1)} + (L-\tau)^{-0.94(1)})$. We see that the exponent governing the power-law behavior is about 1/2 of the equivalent exponent in the space direction, indicating from Eq. (4.21) that the dynamical exponent z must be close to 2. Combining all our estimates for z we find

$$z = 2.0 \pm 0.1 . \tag{6.13}$$

Our estimate for η obtained from Eq. (4.21), including results from the two aspect ratios, is

$$\eta = -0.1 \pm 0.15 . \tag{6.14}$$

This agrees with the inequality Eq. (6.3) $\eta \leq 2 - d$ $(= 0)$, which is possibly satisfied as an equality. Noting that ν is given by Eq. (6.10) and σ^* by Eq. (6.9), this concludes our discussion of the universal properties of the short-range model.

VII. LONG-RANGE COULOMB INTERACTIONS

We shall now include long-range Coulomb interactions. Throughout this section we again take

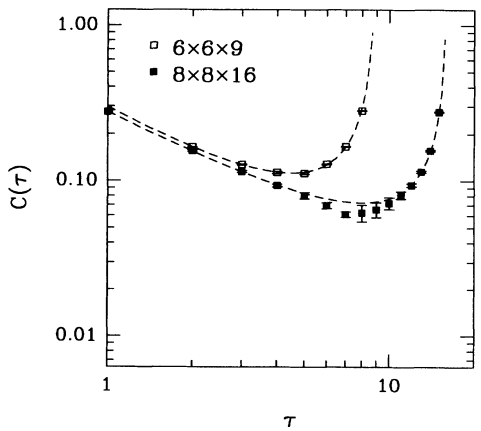

FIG. 12. The correlation function (Green's function) for positive times for short-range interactions for systems of size $6 \times 6 \times 9$ and $8 \times 8 \times 16$, i.e., with aspect ratio 1/4. The calculation was performed at the critical point, $K_c = 0.248$. The dashed line indicates fits to the data. For $L = 6$ the fit is $0.266(4)(\tau^{-1.03(1)} + (L-\tau)^{-1.03(1)})$. For $L = 8$ the fit is $0.256(4)(\tau^{-0.94(1)} + (L-\tau)^{-0.94(1)})$. The data for $\tau > L_\tau/2$ is actually the value of $C_-(L_\tau/2 - \tau)$, as discussed in the text.

$$\tilde{\mu} = \frac{1}{2}, \quad \tilde{\Delta} = \frac{1}{2} , \tag{7.1}$$

but, in addition, take the charge of the bosons to be nonzero. Most of our studies used

$$e^{*2} = \frac{1}{2} , \tag{7.2}$$

but we also have some results for $e^{*2} = 1/4$ as a check that the strength of the Coulomb term is irrelevant. The long-range interactions force us to keep the total boson number fixed, since it has to be compensated by a (fixed) background charge to avoid an energy which is infinite in the thermodynamic limit. We do not, therefore, allow global moves in the time direction (the τ-link variables).

As in the section above on short-range interactions we first discuss what inequalities and estimates there are for the exponents. The result $z = d$, quoted earlier is only applicable to short-range interactions. For a $1/r$ potential, Fisher,[94] has argued that

$$z = 1 . \tag{7.3}$$

A simple way to see this[95] is to compute the characteristic energy, $\Delta\varepsilon$, given by the potential energy at $r = \xi$, i.e., $\Delta\varepsilon = G(r = \xi) \sim \xi^{-1}$, where G is the $1/r$ Coulomb potential. If this is the relevant energy scale in the problem, then $\Delta\varepsilon \sim \xi^{-z}$ with z = 1. This argument is trivially generalized to interactions falling off with some arbitrary power of the distance, $G(r) \sim r^{-\lambda}$, and leads to $z = \lambda$. We expect that this is valid for λ smaller than d, the value for short-range interactions, and that for larger λ, the dynamical exponent sticks at its short-range value, $z = d$. Based on scaling of a renormalized charge Fisher *et al.*[6] derive the inequality

$$z \leq 1 , \tag{7.4}$$

and an argument that the second sound velocity should not diverge at the critical point[10] gives, quite generally,

$$z \geq 1 . \tag{7.5}$$

Hence there is quite strong evidence that $z = 1$ for the $1/r$ interaction. This is convenient for the Monte Carlo work, because, although the computer time per update increases by adding the long-range interaction, the number of lattice points is not so large as for the short-range case because we only have to scale L_τ with the first power of L, rather than its square.

In the section above on short-range range interactions, the inequality $\eta \leq 2-d$ was discussed. This was derived[10] with the assumption that the density of single-particle states in the Bose glass phase is finite at zero energy, an assumption which is no longer correct with $1/r$ interactions.[96,97] In a classical model, called the "Coulomb glass," Efros and Shklovskii[96,97] (ES) argue that the single-particle density of states, $\rho_1(\varepsilon)$, vanishes at $\varepsilon = 0$, due to the "Coulomb gap." Assuming that

$$\rho_1(\varepsilon) \sim \varepsilon^a , \tag{7.6}$$

ES obtain a bound on the density of states for small ε,

$$\rho_1(\varepsilon) \leq C\varepsilon^{d-1} , \tag{7.7}$$

so that

$$a \geq d-1 . \tag{7.8}$$

The value of a in 2D does not seem to be precisely known.[98]

Since the Coulomb glass model is classical, the statistics of the particles does not matter, and so Eq. (7.8) should be applicable to the Bose glass phase, provided quantum fluctuations are unimportant in this region, as is argued for the electron case.[96,97] It is then straightforward to determine the long-time behavior of the Green's function in the Bose glass phase. For $\tau > 0$ we have

$$C(\tau) = \int_0^\infty d\varepsilon e^{-\varepsilon|\tau|}\rho_1(\varepsilon) \sim \frac{1}{\tau^{1+a}} . \tag{7.9}$$

The same argument, together with Eq. (4.21), indicates that at criticality $\rho_1(\varepsilon) \sim \varepsilon^{(d-2+\eta)/z}$. We now assume, following Fisher *et al.*[10], that $\rho_1(\varepsilon)$ at small ε grows as the critical point is approached, in order to match onto the δ-function density of states in the superconducting state. In other words, the density of states exponent is smaller at the critical point than in the Bose glass phase, i.e., $(d-2+\eta)/z \leq a$ or

$$\eta \leq 2 - d + az , \tag{7.10}$$

which, as expected, reduces to Eq. (6.3) for a constant density of states, $a = 0$. The bound $\nu \leq 2/d$, Eq. (6.5), should also be valid in the case of long-range interactions.

We now discuss the results from the simulations. Since there are strong arguments, discussed above, that $z = 1$, we work with systems with shape $L \times L \times L$ with $L =$ 6, 8, 10, and 12. In most cases we perform 3000 MCS for equilibration followed by 3000 MCS with a measurement every 10 MCS. Close to the critical point the number of sweeps was generally larger for the larger sizes. The number of disorder realizations varied from 200 to 1000. As was the case for short-range interactions we carefully check for equilibration by computing the "Hamming distances" discussed in Sec. V.

A. Determination of the critical point

Since $z = 1$, it follows from the discussion after Eq. (4.5) that we should look for the intersections of data for $\rho(0)L$ against K for different lattice sizes. Our results are presented in Fig. 13 for the case of the Ewald-sum form of the potential with $e^{*2} = 1/2$. Clearly the lines cross close to $K = 0.240$ and, more precisely, we estimate the critical coupling to be $K_c = 0.240 \pm 0.003$, quite close to the value for the short-range case. Since all four sizes intersect very close to the same point, Fig. 13 provides strong evidence that $z = 1$, in agreement with the scaling arguments.

An equivalent analysis can be performed with the Green's function form for the potential, Eq. (2.44), with

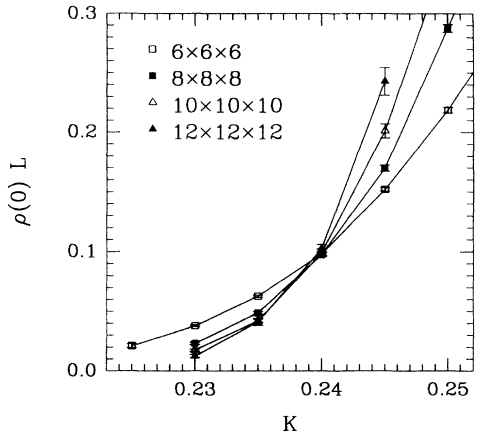

FIG. 13. $\rho(0)L$ for the system sizes indicated, as a function of K. The system sizes indicated correspond to an aspect ratio of 1. The critical point, determined from the intersections, is $K_c = 0.240 \pm 0.003$. The Ewald-sum form of the Coulomb potential was used with $e^{*2} = 1/2$.

$e^{*2} = 1/4$. The two forms of the potential are different on short length scales, and the values of e^{*2} are therefore not directly comparable. Although we do not have enough data for the largest size, $12 \times 12 \times 12$, to perform a conclusive analysis, we can determine the critical coupling to be $K_c \simeq 0.275$, somewhat higher than for the Ewald form, with reasonable certainty.

B. Conductivity

Following the approach used above for the short-range case, we plot, in Fig. 14, the resistivity, $R^*_\square$ in units of R_Q, against frequency at the critical point, $K_c = 0.240$.

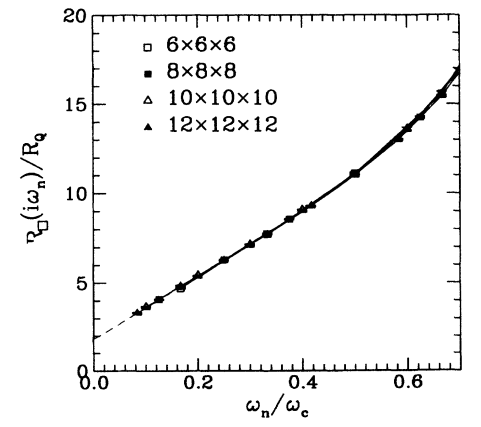

FIG. 14. The resistivity in units of $R_Q = h/(2e)^2$, as a function of ω_n/ω_c, where $\omega_c = 2\pi$. The calculation was done at the critical point, $K = 0.240$. The aspect ratio was in this case 1, and the system sizes shown were as indicated in the figure. $e^{*2} = 1/2$ was used along with the Ewald form for the potential. The dashed line indicates a least squares fit to the points with abscissa less than 0.44 of the form $1.82(2) + 17.84(7)\omega_n/\omega_c$.

This data is for $e^{*2} = 1/2$, with the Ewald method used to evaluate the Coulomb potential. The collapse of the data is excellent, without any correction involving T/ω_n, which was used for the short-range case. This implies that we can interchange the two limits $\omega \to 0$, and $T \to 0$ as expected. As for the short-range case, the data varies linearly with ω_n, implying a Drude form for the conductivity. Making a least squares fit to the data with $\omega_n/\omega_c < 0.44$ we find $R^*_\square/R_Q = 1.82(2)$.

We can now try to investigate the universality of $R^*_\square$ by studying the model with $e^{*2} = 1/4$ and the potential evaluated by the Green's function method. Figure 15 shows the resistivity at the critical point $K_c = 0.275$, along with the data already presented in Fig. 14. We see two interesting things. First, the actual form of the resistivity as a function of frequency is clearly different in the two cases. However, the extrapolation to zero frequency is the same within the uncertainties. For the Green's function potential the best fit is $R^*_\square/R_Q = 1.91(7)$, again for points with abscissa less than 0.44. The agreement between the zero-frequency limit of the two sets of data in Fig. 15 provides strong support for the resistivity being universal at the transition.

We have also studied the effect of the aspect ratio on the resistivity. This is important because the aspect ratio is related to quantities relevant for experiments, as we shall now show. An important concept in mesoscopic physics is the phase coherence length $\xi_{\rm inc}$. This length is expected to diverge as $T \to 0$, and so, at criticality, should be proportional to the Bose glass correlation length, ξ, making the usual assumption that there is only one divergent length scale. To determine how ξ varies as a function of $T \sim L_\tau^{-1}$ note that from finite-size scaling, the finite-size relaxation time ξ_τ at criticality should be proportional to L_τ and so characteristic lengths should scale as $\xi_\tau^{1/z}$. Consequently $\xi_{\rm inc} \sim T^{-1/z}$, which means that the aspect ratio can be expressed as

$$c \equiv \frac{L_\tau}{L^z} \sim \frac{1}{TL^z} \sim \left(\frac{\xi_{\rm inc}}{L}\right)^z ; \qquad (7.11)$$

i.e., it is proportional to a power of the ratio of the phase coherence length to the lattice size. Experiments are generally carried out in the range $L \gg \xi_{\rm inc}$, and so one should view the conductivity as arising from *incoherent* self-averaging of domains whose size is $\xi_{\rm inc}$. In the opposite limit, $L \ll \xi_{\rm inc}$, we expect large variations from sample to sample ("bosonic universal conductance fluctuations"), and the average conductance will not necessarily be the same as that obtained in the regime $L \gg \xi_{\rm inc}$. Thus, the conductivity at zero frequency but finite temperature is given by a scaling function, $\tilde{\sigma}(1/TL^z)$, where the argument is proportional to the aspect ratio. The experimental situation corresponds to the limit of zero aspect ratio, whereas the simulations are done for a finite value.

We have therefore performed calculations for two other aspect ratios, 1/2 and 3/2 respectively. In both cases we used the Ewald form of the potential with $e^{*2} = 1/2$. In order to obtain scaling plots for aspect ratios different from 1 it is necessary to include corrections of the form $1/L^2$. Including this correction term, our estimates for $R^*_\square$ agree with those for aspect ratio unity, within the errors. Thus any dependence of $R^*_\square$ on aspect ratio seems to be quite small.

In conclusion, we estimate the universal conductivity at the critical point from all our data to be

$$R^*_\square = (1.82 \pm 0.20) R_Q \ , \quad \sigma^* = (0.55 \pm 0.06) G_Q \ . \qquad (7.12)$$

No dependence on the aspect ratio, the microscopic form of the potential, the strength of the Coulomb interaction, or particle density was observed.

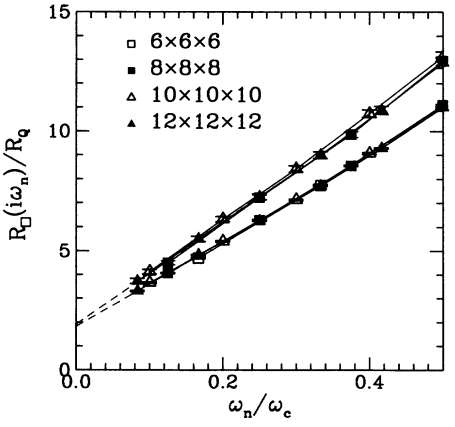

FIG. 15. The resistivity in units of $R_Q = h/(2e)^2$, as a function of ω_n/ω_c, where $\omega_c = 2\pi$. For the upper curve the Green's-function form of the potential was used with $e^{*2} = 1/4$, and an aspect ratio of 1. The calculation was done at the critical point for this potential, $K = 0.275$. The dashed line indicates a least squares fit to the points with abscissa less than 0.44 of the form $1.91(7) + 21.5(3)\omega_n/\omega_c$. The lower curve is the results from the Ewald form of the potential from Fig. 14. Although the results for the two forms of the potential differ at finite frequency, they appear to extrapolate to the same value in the dc limit, as expected since the dc resistivity is predicted to be universal.

C. Wave-vector-dependent compressibility

Because of the long-range interactions, the system is incompressible. As a result the wave-vector-dependent compressibility should vary at criticality as $\kappa(k) \sim k$ from Eq. (3.18) with $z = 1$. Figure 16 shows the data at the critical point $K_c = 0.240$, for aspect ratio 1, and the Ewald form of the potential with $e^{*2} = 1/2$. The solid lines shown are cubic splines fitted to the data points. The data for small k seems to be roughly linear, as expected if $z = 1$ but one would need substantially smaller wave vectors to draw a firm conclusion.

Similar results results were obtained for aspect ratios 1/2 and 3/2.

D. Exponent ν

To determine the correlation length exponent we try to collapse the data in a scaling plot of $\rho(0)L$ versus $\delta L^{1/\nu}$,

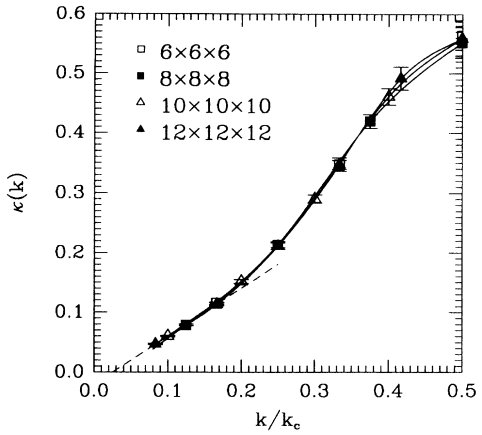

FIG. 16. The compressibility at the critical point for the same model as in Fig. 14, as a function of wave vector, for different system sizes, where $k_c = 2\pi$ is the lattice cutoff. As expected in Coulomb systems, the compressibility appears to vanish as $k \to 0$. The solid lines are spline fits to the data points, and $k_c = 2\pi$. Also indicated by a dashed line is a tentative fit to the low-frequency part with abscissa less than 0.19 of the form $-0.020(2) + 0.8(2)k/k_c$.

based on Eq. (4.4). Figure 17 shows the data for $\nu = 0.90$ and $K_c = 0.240$, with aspect ratio 1, and the Ewald form of the potential with $e^{*2} = 1/2$. By considering all our data we estimate

$$\nu = 0.9 \pm 0.15 \ . \tag{7.13}$$

The estimate of ν is again consistent with the inequality of Chayes *et al.*,[89] $\nu \geq 2/d$, being satisfied as an equality.

E. Correlation functions

Assuming $z = 1$ we expect the spatial correlation functions to have an asymptotic form of $C_x(r) \sim r^{-y_x}$ with

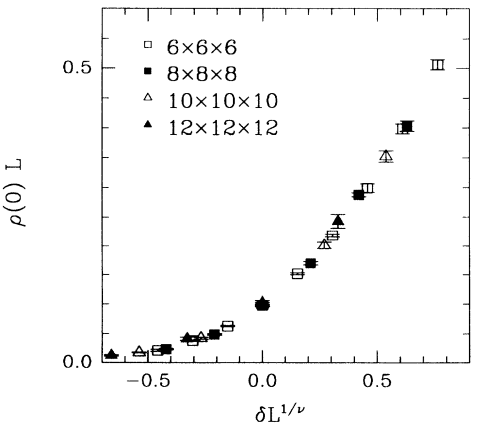

FIG. 17. Scaling plot of $\rho(0)L$ versus $\delta L^{1/\nu}$, where δ is the reduced coupling constant $(K - K_c)/K_c$ and L is the linear system size. The model is the same as in Fig. 14. The parameters used in the plot are $K_c = 0.240$, $\nu = 0.90$.

$y_x = 1 + \eta$; see Eq. (4.21). We have calculated the equal-time correlation functions for three different system sizes, $L \times L \times L$ with $L = 8, 10$, and 12. The Ewald form of the potential was used with $e^{*2} = 1/2$, and the calculation was performed at the critical point $K_c = 0.240$. Despite there being quite a lot of noise in the data at large arguments, we can fit to the form in Eq. (6.11) with the result $y_x = 1.8 \pm 0.4$. Assuming that $z = 1$ this then tells us that $\eta = 0.8 \pm 0.4$ in agreement with the previously derived inequality, Eq. (7.10), $\eta \leq az$, with $a \geq 1$.

In principle, the time-dependent correlation functions can also be determined. However, unlike the equal-time correlation functions, these involve injecting an extra particle and then destroying it at a later time. Long-range interactions complicate the simulation of this correlation function and we have not attempted it. Hence we cannot independently confirm the value $z = 1$ of the dynamical exponent found in the scaling of $\rho(0)L^z$, but believe it to be accurate. Similarly, we have not attempted to obtain the time decay of the correlation functions deep in the Bose glass phase, which could give us information on the Coulomb gap exponent, a in Eq. (7.6).

VIII. DISCUSSION

We have investigated universal properties of the $T = 0$ Bose glass to superfluid transition in two dimensions both for particles with short-range interactions and for particles with long-range $(1/r)$ Coulomb interactions. We used a version of the path-integral approach which corresponds to including only phase fluctuations of the condensate.

For the case of long-range Coulomb interactions we find $\nu = 0.90 \pm 0.15$, $\eta = 0.8 \pm 0.4$, $z \simeq 1.0$, and $\sigma^* = (0.55 \pm 0.06)\, G_Q$ where $G_Q^{-1} \equiv R_Q \equiv h/(2e)^2 \approx 6.45$ kΩ. This model should be in the right universality class to describe the superconductor-insulator transition in disordered thin films. Experimental results[25,26,28,29,31,39] do not show much support for the universality of σ^*, the values of σ^*/G_Q varying from about 0.6 to 2. However, it is possible that many of these experiments were not at sufficiently low temperature to probe the critical regime. We are not aware of any other theoretical calculations with which to compare our results.

For the case of short-range interactions we find $\nu = 0.9 \pm 0.1$, $\eta = -0.10 \pm 0.15$, and $z = 2.0 \pm 0.10$. The universal conductivity is in this case $\sigma^* = (0.14 \pm 0.03) G_Q$. These results are in reasonable accord with those of Runge,[57] who studied a hard-core boson model on small lattices of size up to 4×4 by diagonalization, and obtained $\nu = 1.4 \pm 0.3$ and $z = 1.95 \pm 0.25$. He also found $\sigma^*/G_Q = 0.16 \pm 0.01$, in agreement with our estimate, though the error bar may be rather optimistic, since different assumptions for the finite-size corrections led to significantly different values.

Both for the short-range and long-range interactions, our results for ν are consistent with the rigorous inequality[89,90] $\nu \geq 2/d$, where d is the number of dimensions in which the systems is disordered ($d = 2$ here), being satisfied as an *equality*. This result has also been shown to

occur in certain models with correlated disorder,[93] and it would be interesting to see if it is a rather general property at quantum transitions with quenched disorder.

Since this work was completed, two groups have reported results for the short-range model which differ from ours. Batrouni *et al.*[60] have performed world-line quantum Monte Carlo simulations directly on the boson Hubbard model. They find $\sigma^* = (0.45 \pm 0.07)G_Q$, but do not report values for the exponents. We do not have an explanation for this discrepancy, though we note that their data for $L^2\rho(0)$ do not splay out in the insulating phase, $K < K_c$, as do ours (see Fig. 5), which makes the location of the critical point harder.

Results which are totally different from ours and also different from those of Batrouni *et al.*[60] have been found by Makivić *et al.*[61] who performed world-line quantum Monte Carlo simulations on a hard-core Bose system with short range interactions finding $\sigma^* = (1.2 \pm 0.2)G_Q$, with $z = 0.5 \pm 0.05$ and $\nu = 2.2 \pm 0.2$. The value of the dynamical exponent z found by Makivić *et al.* is surprisingly small; we are not aware of any other situations where $z < 1$. The finite-size scaling analysis was therefore performed with samples which were small in the τ direction, and so one might be concerned that the system is close to the classical transition, and the full quantum regime might not have been reached. This concern is reinforced if one notes that the critical coupling differed by a factor of 2 for the two temperatures that were studied. Makivić *et al.*[61] propose that the difference between their results and ours is that amplitude fluctuations, neglected in our model but included in the boson Hamiltonians, are relevant, and so the two models are in different universality classes. While this idea certainly cannot be ruled out, we do not yet feel that it has been conclusively demonstrated. First of all, the only evidence for it is the numerical results, about which we have some reservations discussed above. It would be more compelling if there were additional evidence, such as a calculation of the exponent for amplitude fluctuations, showing that it is indeed relevant in the renormalization group sense. Furthermore, this explanation does not explain the differences between the results of Makivić *et al.*[61] and those of Batrouni *et al.*[60] and Runge,[57] which also included amplitude fluctuations.

For the future, it would be very interesting to study the field-tuned transition[37,38] by Monte Carlo simulations, since this is expected to be in a different universality class[94] from the disorder-tuned transition discussed here. The problem is that one needs to find a representation of the problem in terms of a *real* classical $(D+1)$-dimensional effective Hamiltonian which incorporates both the magnetic field and lack of microscopic particle-hole symmetry. Unfortunately, the phase representation, Eq. (2.27), though it can be generalized to include a field and is still real for the particle-hole symmetric case, is complex in the absence of particle-hole symmetry, and the link representation used here becomes complex in the presence of a field, as can be seen from Eq. (2.35). We are therefore unaware of any representation of the problem suitable for Monte Carlo simulations.

ACKNOWLEDGMENTS

We thank M. P. A. Fisher, A. Hebard, R. Dynes, J. M. Valles, A. M. Goldman, M.-C. Cha, K. Runge, N. Trivedi, G. Zimanyi, I. Affleck, J. Gan, M. Gingras, H. J. Schulz, R. Scalettar, and S. Kivelson for a large number of valuable suggestions and discussions. A.P.Y. and E.S.S. acknowledge the kind hospitality of Ecole Normale Supérieure, Paris, and CEA, Saclay, where a major part of this work was done, as well as generous CPU-time allocations at the CCVR, Saclay, and San Diego Supercomputer Cray facilities. E.S.S. also acknowledges support from the Danish Natural Research Council, as well as from NSERC and CIAR of Canada. M.W. is supported by the Swedish Natural Science Research Council. S.M.G. is supported by DOE Grant No. DE-FG02-90ER45427 and NCSA Grant No. DMR-910014N. A.P.Y. and E.S.S. are supported by NSF Grant No. DMR-91-11576.

APPENDIX

In this appendix we derive Eq. (2.37) which gives the action in the presence of disorder and a finite chemical potential, both of which break particle-hole symmetry. Starting with the boson Hubbard model in Eq. (2.2) we form the coherent state path integral

$$Z = \int D[\Phi] e^{-S}, \tag{A1}$$

where the action is given by

$$S = \int_0^\beta d\tau \left\{ \sum_{\mathbf{r}} \left[\Phi_{\mathbf{r}}^* \partial_\tau \Phi_{\mathbf{r}} + \frac{U}{2} |\Phi_{\mathbf{r}}|^4 - (\mu + v_{\mathbf{r}} - zt)|\Phi_{\mathbf{r}}|^2 \right] - t \sum_{\langle \mathbf{r},\mathbf{r}' \rangle} (\Phi_{\mathbf{r}}^* \Phi_{\mathbf{r}'} + \Phi_{\mathbf{r}'}^* \Phi_{\mathbf{r}}) \right\}, \tag{A2}$$

in which the $\Phi_{\mathbf{r}}(\tau)$ are complex classical fields. Next we write Φ in terms of its amplitude and phase,

$$\Phi_{\mathbf{r}} = \sqrt{\rho_{\mathbf{r}}} e^{i\theta_{\mathbf{r}}} , \tag{A3}$$

and expand $\rho_{\mathbf{r}}$ about its equilibrium value, $n_{\mathbf{r}}$,

$$\rho_{\mathbf{r}} = n_{\mathbf{r}} + \delta\rho_{\mathbf{r}} . \tag{A4}$$

Close to the critical point, the phase θ will be slowly varying in position and imaginary time. We expand the action

up to second order in small quantities regarding $\partial_\tau \Phi$ and $\delta\rho$ as first order and $1-\cos(\theta_{\mathbf{r}}-\theta_{\mathbf{r}'})$ as second order. The result is

$$S=\int_0^\beta d\tau\Bigg\{\sum_{\mathbf{r}}\left[\frac{U}{2}n_{\mathbf{r}}^2-(\mu+v_{\mathbf{r}}-zt)n_{\mathbf{r}}\right]-2t\sum_{\langle\mathbf{r},\mathbf{r}'\rangle}\sqrt{n_{\mathbf{r}}n_{\mathbf{r}'}}$$

$$+\frac{U}{2}\sum_{\mathbf{r}}\delta\rho_{\mathbf{r}}^2-2t\sum_{\langle\mathbf{r},\mathbf{r}'\rangle}\left[\frac{\delta\rho_{\mathbf{r}}\delta\rho_{\mathbf{r}'}}{2\sqrt{n_{\mathbf{r}}n_{\mathbf{r}'}}}-\frac{1}{8}\left\{\left(\frac{\delta\rho_{\mathbf{r}}}{n_{\mathbf{r}}}\right)^2+\left(\frac{\delta\rho_{\mathbf{r}'}}{n_{\mathbf{r}'}}\right)^2\right\}\sqrt{n_{\mathbf{r}}n_{\mathbf{r}'}}\right]$$

$$+\sum_{\mathbf{r}}\delta\rho_{\mathbf{r}}\left(-i\partial_\tau\theta_{\mathbf{r}}+n_{\mathbf{r}}U-\mu-v_{\mathbf{r}}+zt\right)-2t\sum_{\langle\mathbf{r},\mathbf{r}'\rangle}\left[\frac{1}{2}\sqrt{\frac{n_{\mathbf{r}'}}{n_{\mathbf{r}}}}\delta\rho_{\mathbf{r}}+\frac{1}{2}\sqrt{\frac{n_{\mathbf{r}}}{n_{\mathbf{r}'}}}\delta\rho_{\mathbf{r}'}\right]$$

$$+2t\sum_{\langle\mathbf{r},\mathbf{r}'\rangle}\sqrt{n_{\mathbf{r}}n_{\mathbf{r}'}}\left[1-\cos(\theta_{\mathbf{r}}-\theta_{\mathbf{r}'})\right]-i\sum_{\mathbf{r}}n_{\mathbf{r}}\partial_\tau\theta_{\mathbf{r}}\Bigg\}\,, \tag{A5}$$

where we have used $\int_0^\beta \partial\rho_{\mathbf{r}}/\partial\tau=\rho_{\mathbf{r}}(\beta)-\rho_{\mathbf{r}}(0)=0$ because of periodic boundary conditions in the τ direction. The terms involving t in line 1 of Eq. (A5) cancel for a pure system. With disorder they just give an unimportant additive constant. For a pure system, the terms involving t in line 2 give rise to an additional contribution to U and also a nearest-neighbor interaction energy. With disorder, random components of these occur too. All these extra terms could have been included in the original boson Hamiltonian without changing the universality class. They do not change the symmetry, as long as the model has a random site energy, and so would be generated by a renormalization group transformation even if not included in the starting Hamiltonian. The terms proportional to t in line 3 cancel for a pure system, and, with disorder, just give an additional contribution to the random potential. The coefficient of the cosine term in line 4 is random when the system is disordered. This corresponds to a random hopping in the original Hamiltonian which again does not change the symmetry and would be generated by a renormalization group transformation. Neglecting these irrelevant terms, the action becomes

$$S=\int_0^\beta d\tau\Bigg\{\sum_{\mathbf{r}}\left[\frac{U}{2}n_{\mathbf{r}}^2-(\mu+v_{\mathbf{r}})n_{\mathbf{r}}+\frac{U}{2}\delta\rho_{\mathbf{r}}^2+\delta\rho_{\mathbf{r}}\left(-i\partial_\tau\theta_{\mathbf{r}}+n_{\mathbf{r}}U-\mu-v_{\mathbf{r}}\right)\right]$$

$$+2tn_0\sum_{\langle\mathbf{r},\mathbf{r}'\rangle}\left[1-\cos(\theta_{\mathbf{r}}-\theta_{\mathbf{r}'})\right]-i\sum_{\mathbf{r}}n_{\mathbf{r}}\partial_\tau\theta_{\mathbf{r}}\Bigg\}\,. \tag{A6}$$

Now complete the square on $\delta\rho$, and redefine $2tn_0$ to be t. This gives

$$S=\int_0^\beta d\tau\Bigg\{\sum_{\mathbf{r}}\left[-\frac{(\mu+v_{\mathbf{r}})^2}{2U}-i\frac{(\mu+v_{\mathbf{r}})}{U}\partial_\tau\theta_{\mathbf{r}}+\frac{1}{2U}(\partial_\tau\theta_{\mathbf{r}})^2\right]+t\sum_{\langle\mathbf{r},\mathbf{r}'\rangle}\left[1-\cos(\theta_{\mathbf{r}}-\theta_{\mathbf{r}'})\right]\Bigg\}\,. \tag{A7}$$

Note that for the special case of $v_{\mathbf{r}}=0$ and μ/U an integer, the term involving $\int_0^\beta \partial_\tau\theta_{\mathbf{r}}=\theta_{\mathbf{r}}(\beta)-\theta_{\mathbf{r}}(0)$ does not contribute because $\theta_{\mathbf{r}}(\beta)-\theta_{\mathbf{r}}(0)=2\pi\times$ integer.

Next form the path-integral representation of the quantum rotor model,

$$H_{\mathrm{qr}}=T+V, \tag{A8}$$

$$T\equiv\frac{U}{2}\sum_{\mathbf{r}}\left(\frac{1}{i}\frac{\partial}{\partial\theta_{\mathbf{r}}}\right)^2+i\sum_{\mathbf{r}}(\mu+v_{\mathbf{r}})\left(\frac{\partial}{\partial\theta_{\mathbf{r}}}\right), \tag{A9}$$

$$V\equiv-\sum_{\langle\mathbf{r},\mathbf{r}'\rangle}t\cos(\theta_{\mathbf{r}}-\theta_{\mathbf{r}'})\,. \tag{A10}$$

Following essentially the inverse of the steps that led from Eq. (2.4) to Eq. (2.23) we find that the action is the same as in Eq. (A7) above. Thus the long-wavelength properties of the quantum rotor Hamiltonian, Eq. (A8), should be the same as those of the boson Hubbard model, Eq. (2.2).

Proceeding as before, but starting from Eq. (A8) rather than Eq. (2.4), we arrive at the analog of Eq. (2.16),

$$T_j=\prod_{\mathbf{r}}\left\langle\theta_{\mathbf{r}}(\tau_{j+1})\left|\exp\left[\frac{\Delta\tau U}{2}\frac{\partial^2}{\partial\theta_{\mathbf{r}}^2}+i\Delta\tau\,(\mu+v_{\mathbf{r}})\left(\frac{\partial}{\partial\theta_{\mathbf{r}}}\right)\right]\right|\theta_{\mathbf{r}}(\tau_j)\right\rangle\,. \tag{A11}$$

Inserting a complete set of angular momentum eigenstates, we have

$$T_j = \exp\left\{-\frac{\Delta\tau U}{2}\left[J^\tau_{\mathbf{r}}(\tau_j)\right]^2 - \Delta\tau(\mu + v_{\mathbf{r}})J^\tau_{\mathbf{r}}(\tau_j)\right\}. \tag{A12}$$

Next we plug Eq. (A12) into the analog of Eq. (2.19). Again making the Villain approximation and using the Poisson summation formula, we arrive exactly at Eq. (2.37).

[1] E. Abrahams, P. W. Anderson, D. C. Licciardello, and T. V. Ramakrishnan, Phys. Rev. Lett. **42**, 673 (1979).

[2] P. A. Lee and T. V. Ramakrishnan, Rev. Mod. Phys. **57**, 287 (1985) and references therein.

[3] As we shall discuss extensively in this paper, the long-distance properties of superconductivity can, at least to some extent, be described in terms of (repulsively interacting) bosons. It thus appears that fermions with repulsive interactions are always localized (i.e., insulating at $T = 0$) in $d = 2$, whereas bosons can (super)conduct if the disorder is not too strong. Unlike the situation for fermions, the repulsive interaction is *essential* for bosons; otherwise they all condense into the lowest localized state. Thus it appears that weak repulsion actually tends to *delocalize* the bosons; see e.g., G. Batrouni and R. T. Scalettar, Phys. Rev. B **46** 9051 (1992); W. Krauth, N. Trivedi, and D. Ceperley, Phys. Rev. Lett. **67**, 2307 (1991).

[4] The criterion for weak disorder being relevant is[91] $\nu < 2/d$, where ν is the correlation length exponent of the pure system and d the dimensionality. At the Kosterlitz-Thouless transition (Ref. 5), $\nu = \infty$, corresponding to an exponential, rather than power-law, divergence, and so disorder is highly irrelevant.

[5] J. M. Kosterlitz and D. J. Thouless, J. Phys. C **6**, 1181 (1973); J. M. Kosterlitz, J. Phys. C **7**, 1046 (1974).

[6] M. P. A. Fisher, G. Grinstein, and S. M. Girvin, Phys. Rev. Lett. **64**, 587 (1990).

[7] X. G. Wen and A. Zee, Int. J. Mod. Phys. B **4**, 437 (1990).

[8] S. Chakravarty, G.-L. Ingold, S. Kivelson, and A. Luther, Phys. Rev. Lett. **56**, 2303 (1986); S. Chakravarty, S. Kivelson, G. T. Zimanyi, and B. I. Halperin, Phys. Rev. B **35**, 7256 (1987).

[9] E. S. Sørensen, M. Wallin, S. M. Girvin, and A. P. Young, Phys. Rev. Lett. **69**, 828 (1992).

[10] M. P. A. Fisher, P. B. Weichman, G. Grinstein, and D. S. Fisher, Phys. Rev. B **40**, 546 (1989).

[11] J. Pearl, Appl. Phys. Lett. **5**, 65 (1964); in *Low Temperature Physics LT9*, edited by J. D. Gaunt, D. O. Edwards, F. J. Milford, and M. Yaqub (Plenum, New York, 1965), p. 566.

[12] B. I. Halperin and D. R. Nelson, J. Low Temp. Phys. **36**, 599 (1979).

[13] S. Doniach and B. A. Huberman, Phys. Rev. Lett. **42**, 1169 (1979).

[14] M. R. Beasley, J. E. Mooij, and T. P. Orlando, Phys. Rev. Lett. **42**, 1165 (1979).

[15] For a review see W. J. Skocpol and M. Tinkham, Rep. Prog. Phys. **38**, 1049 (1975).

[16] A. F. Hebard and A. T. Fiory, Phys. Rev. Lett. **44**, 291 (1980); **50**, 1603 (1983); A. T. Fiory and A. F. Hebard, Phys. Rev. B **25**, 2073 (1982); A. T. Fiory, A. F. Hebard, and W. I. Glaberson, *ibid.* **28**, 5075 (1983).

[17] K. Epstein, A. M. Goldman, and A. M. Kadin, Phys. Rev. Lett. **47**, 534 (1981); Phys. Rev. B **26**, 3950 (1982); A. M. Kadin, A. M. Goldman, and K. Epstein, Phys. Rev. B **27**, 6691 (1983).

[18] L. G. Aslamazov and A. I. Larkin, Phys. Lett. **26A**, 238 (1968).

[19] J. E. Mooij, in *Advances in Superconductivity*, edited by B. Deaver and J. Ruvalds (Plenum Press, New York, 1983), p. 433; in *Percolation, Localization, and Superconductivity*, edited by A. M. Goldman and S. A. Wolf (Plenum Press, New York, 1984), p. 325.

[20] J. W. Hsu and A. Kapitulnik, Phys. Rev. B **45**, 4819 (1992).

[21] A. E. Rana and S. M. Girvin, Phys. Rev. B **48**, 360 (1993).

[22] M. Ma, B. I. Halperin, and P. A. Lee, Phys. Rev. B **34**, 3136 (1986).

[23] M. A. Paalanen, A. F. Hebard, and R. R. Ruel, Phys. Rev. Lett. **69**, 1604 (1992).

[24] For a review of the experimental situation see Y. Liu and A. M. Goldman (unpublished).

[25] D. B. Haviland, Y. Liu, and A. M. Goldman, Phys. Rev. Lett. **62**, 2180 (1989).

[26] Y. Liu, K. A. McGreer, B. Nease, D. B. Haviland, G. Martinez, J. W. Halley, and A. M. Goldman, Phys. Rev. Lett. **67**, 2068 (1991).

[27] H. M. Jaeger, D. B. Haviland, B. G. Orr, and A. M. Goldman, Phys. Rev. B **40**, 182 (1989).

[28] T. Wang, K. M. Beauchamp, D. D. Berkley, B. R. Johnson, J.-X. Liu, J. Zhang, and A. M. Goldman. Phys. Rev. B **43**, 8623 (1991).

[29] T. Wang, K. M. Beauchamp, A. M. Mack, N. Chandrasekhar, N. E. Israeloff, G. C. Spalding, and A. M. Goldman, Phys. Rev. B **47**, 11619 (1993).

[30] S. Tanda, S. Ohzeki, and T. Nakayama, Phys. Rev. Lett. **69**, 530 (1992).

[31] S. J. Lee and J. B. Ketterson, Phys. Rev. Lett. **64**, 3078 (1990).

[32] L. J. Geerligs, M. Peters, L. E. M. de Groot, A. Verbruggen, and J. E. Mooij, Phys. Rev. Lett. **63**, 326 (1989).

[33] H. S. J. van der Zant, L. J. Geerligs, and J. E. Mooij, Europhys. Lett. **19**, 541 (1992); H. S. J. van der Zant, F. C. Fritschy, W. J. Elion, L. J. Geerligs, and J. E. Mooij, Phys. Rev. Lett. **69**, 2971 (1992).

[34] R. Fazio and G. Schön, in *Proceedings of the International Conference on Transport Properties of Superconductors*, edited by R. Nicolsky (World Scientific, Singapore, 1990), p. 298.

[35] R. Fazio and G. Schön, Phys. Rev. B **43**, 5307 (1991).

[36] P. A. Bobbert, R. Fazio, G. Schön, and G. T. Zimanyi, Phys. Rev. B **41**, 4009 (1990).

[37] A. F. Hebard and M. A. Paalanen, Phys. Rev. Lett. **65**, 927 (1990).

[38] A. F. Hebard and M. A. Paalanen, Helv. Phys. Acta **65**, 197 (1992).

[39] Y. Liu, K. A. McGreer, B. Nease, D. B. Haviland, G. Martinez, J. W. Halley, and A. M. Goldman, Phys. Rev. Lett. **67**, 2068 (1991).
[40] A. F. Hebard and M. A. Paalanen, Phys. Rev. Lett. **54**, 2155 (1985).
[41] R. C. Dynes, A. E. White, J. M. White, and J. P. Garno, Phys. Rev. Lett. **57**, 2195 (1986).
[42] J. M. Valles, R. C. Dynes, and J. P. Garno, Phys. Rev. B **40**, 6680 (1989); Phys. Rev. Lett. **69**, 3567 (1992).
[43] A. Gold, Z. Phys. B **52**, 1 (1983); **81**, 155 (1990).
[44] T. Giamarchi and H. J. Schulz, Europhys. Lett. **3**, 1287 (1987); Phys. Rev. B **37**, 325 (1988).
[45] M. P. A. Fisher and G. Grinstein, Phys. Rev. Lett. **60**, 208 (1988).
[46] D. S. Fisher and M. P. A. Fisher, Phys. Rev. Lett. **61**, 1847 (1988).
[47] M. P. A. Fisher and D. H. Lee, Phys. Rev. B **39**, 2756 (1989).
[48] P. B. Weichman, Phys. Rev. B **38**, 8739 (1988); P. B. Weichman and K. Kim, Phys. Rev. B **40**, 813 (1989).
[49] G. G. Batrouni, R. T. Scalettar, and G. T. Zimanyi, Phys. Rev. Lett. **65**, 1765 (1990).
[50] W. Krauth and N. Trivedi, Europhys. Lett. **14**, 627 (1991).
[51] R. T. Scalettar, G. G. Batrouni, and G. T. Zimanyi, Phys. Rev. Lett. **66**, 3144 (1991).
[52] W. Krauth, N. Trivedi, and D. Ceperley, Phys. Rev. Lett. **67**, 2307 (1991).
[53] K. G. Singh and D. S. Rokhsar, Phys. Rev. B **46**, 3002 (1992).
[54] M.-C. Cha, M. P. A. Fisher, S. M. Girvin, M. Wallin, and A. P. Young, Phys. Rev. B **44**, 6883 (1991).
[55] S. M. Girvin, M. Wallin, E. S. Sørensen, and A. P. Young, Phys. Scr. T **42**, 189 (1992).
[56] S. M. Girvin, M. Wallin, M.-C. Cha, M. P. .A. Fisher, and A. P. Young, Prog. Theor. Phys. Suppl. **107**, 135 (1992).
[57] K. Runge, Phys. Rev. B **45**, 13136 (1992).
[58] E. S. Sørensen, Ph.D. thesis, University of California Santa Cruz, 1992.
[59] A. P. Kampf and G. T. Zimanyi, Phys. Rev. B **47**, 279 (1993).
[60] G. G. Batrouni, B. Larson, R. T. Scalettar, J. Tobochnik, and J. Wang, Phys. Rev. B **48**, 9628 (1993).
[61] M. Makivić, N. Trivedi, and S. Ullah, Phys. Rev. Lett. **71**, 2307 (1993).
[62] M. H. W. Chan, K. I. Blum, S. Q. Murphy, G. K. S. Wong, and J. D. Reppy, Phys. Rev. Lett. **61**, 1950 (1988).
[63] G. K. S. Wong, P. A. Crowell, H. A. Cho, and J. D. Reppy, Phys. Rev. Lett. **65**, 2410 (1990).
[64] D. R. Nelson and V. M. Vinokur, Phys. Rev. Lett. **68**, 2398 (1992).
[65] M. Wallin and S. M. Girvin, Phys. Rev. B **47**, 14642 (1993).
[66] M. P. A. Fisher, Phys. Rev. Lett. **62**, 1415 (1989).
[67] S. Doniach, Phys. Rev. B 24, 5063 (1981); R. M. Bradley and S. Doniach, Phys. Rev. B **30**, 1138 (1984).
[68] J. Villain, J. Phys. (Paris) **36**, 581 (1975).
[69] While it is clear that the universality class will not change if the anisotropy among the different lattice directions is finite, one might possibly worry that crossover to some new behavior could occur in the limit when the anisotropy tends to infinity, as happens here. However, there is at least one model, the one-dimensional (quantum) Ising model in a transverse field, which can be mapped on to the classical (1+1)- dimensional classical Ising model in the limit of infinite anisotropy, and which can be solved exactly. One finds, P. Pfeuty, Ann. Phys. (N.Y.) **27**, 79 (1970), that the critical behavior of the quantum problem is the *same* as that of the isotropic classical model. It is therefore reasonable to assume here that no change in critical behavior occurs in the infinitely anisotropic limit.
[70] J. V. José, L. P. Kadanoff, S. Kirkpatrick, and D. R. Nelson, Phys. Rev. B **16**, 1217 (1977).
[71] Statistical particle-hole symmetry occurs when $\tilde{\mu} = n/2$ with n an integer. Microscopic particle-hole symmetry, which means that Hamiltonian is invariant under $J^\tau \to -J^\tau$ for a single sample, occurs when there is no disorder and $\tilde{\mu}$ is an integer (or a half-integer); i.e., the boson filling is an integer (or a half-integer). The Hamiltonian in the phase representation is only real for no disorder and integer filling.
[72] M. P. A. Fisher, Physica A **177**, 553 (1991).
[73] H. Totsuji, Phys. Rev. B **17**, 399 (1978).
[74] D. S. Fisher, B. I. Halperin, and R. Morf, Phys. Rev. B **20**, 4692 (1979).
[75] See, e.g., M. E. Fisher, in *Critical Phenomena*, Vol. 186 of *Lecture Notes in Physics*, edited by F. J. W. Hahne (Springer, Berlin, 1983), p. 1.
[76] D. Stauffer, M. Ferer, and M. Wortis, Phys. Rev. Lett. **29**, 345 (1972).
[77] A. Aharony, Phys. Rev. B **9**, 2107 (1974).
[78] P. C. Hohenberg, A. Aharony, B. I. Halperin, and E. D. Siggia, Phys. Rev. B **13**, 2986 (1976).
[79] A. Aharony, Phys. Rev. B **13**, 3081 (1976).
[80] K. Kim and P. B. Weichman, Phys. Rev. B **43**, 13583 (1991).
[81] M. E. Fisher, M. N. Barber, and D. Jasnow, Phys. Rev. B **8**, 111 (1973).
[82] J. Hertz, Phys. Scr. T **10**, 1 (1985).
[83] D. R. Nelson and M. J. Kosterlitz, Phys. Rev. Lett. **39**, 1201 (1977).
[84] V. Privman, in *Finite Size Scaling and Numerical Simulation of Statistical Systems*, edited by V. Privman (World Scientific, Singapore, 1990), p. 1.
[85] R. P. Feynman, *Statistical Mechanics* (Addison-Wesley, Reading, MA, 1972), Chap. 11.
[86] R. N. Bhatt and A. P. Young, Phys. Rev. B **37**, 5606 (1988).
[87] It might be thought, from the definitions Eqs. (4.14) and (4.16), that $C_+(\tau) = [C_-(\tau)]^*$. However, this is not correct. Both correlation functions are real, but different from each other except when there is statistical particle-hole symmetry. The point is that, except with integer filling and no disorder (for which there is exact particle-hole symmetry), the Hamiltonian is not real in the phase representation, and so taking the complex conjugate is not trivial.
[88] K. Binder and A. P. Young, Rev. Mod. Phys. **58**, 801 (1986).
[89] J. T. Chayes, L. Chayes, D. S. Fisher, and T. Spencer, Phys. Rev. Lett. **57**, 2999 (1986).
[90] J. T. Chayes, L. Chayes, D. S. Fisher, and T. Spencer, Commun. Math. Phys. **120**, 501 (1989).
[91] A. B. Harris, J. Phys. C **7**, 1671 (1974).
[92] The horizontal axis is really $\omega_n/\omega_c - \alpha L^{-2}(\omega_c/\omega_n)$, where $\alpha = 0.179$ and $\omega_c = 2\pi$ is the lattice cutoff. The correction factor involving α is proportional to T/ω_n as discussed in the text. The value of α is considerably smaller than the best fit for the case of no disorder (Ref. 54) which gave $\alpha = 0.74$. The data scale fairly well even for $\alpha = 0$ and this fit gives a very similar value of σ^*. As discussed in the text, it is expected that the correct value is $\alpha = 0$.

[93] A. Weinrib and B. I. Halperin, Phys. Rev. B **27**, 413 (1983).
[94] M. P. A. Fisher, Phys. Rev. Lett. **65**, 923 (1990).
[95] M. P. A. Fisher (private communication).
[96] B. I. Shklovskii and A. L Efros, *Electron Properties of Doped Semiconductors* (Springer-Verlag, New York, 1984).
[97] A. L. Efros and B. I. Shklovskii, in *Electron-Electron Interactions in Disordered Systems*, edited by A. L. Efros and M. Pollak (North-Holland, Amsterdam, 1985).
[98] J. D. Davies, P. A. Lee, and T. M. Rice, Phys. Rev. Lett. **49**, 758 (1982).